# Biosynthetic, biomimetic, and self-assembled vascularized Organ-on-a-Chip systems

Anna Fritschen, Andreas Blaeser

Institute for BioMedical Printing Technology
Technical University of Darmstadt
fritschen@idd.tu-darmstadt.de, blaeser@idd.tu-darmstadt.de

Magdalenenstr. 2
64289 Darmstadt
Germany

# Abstract

Organ-on-a-Chip (OOC) devices have seen major advances in the last years with respect to biological complexity, physiological composition and biomedical relevance. In this context, integration of vasculature has proven to be a crucial element for long-term culture of thick tissue samples as well as for realistic pharmacokinetic, toxicity and metabolic modelling. With the emergence of digital production technologies and the reinvention of existing tools, a multitude of design approaches for guided angio- and vasculogenesis is available today. The underlying production methods can be categorized into biosynthetic, biomimetic and self-assembled vasculature formation. The diversity and importance of production approaches, vascularization strategies as well as biomaterials and cell sourcing are illustrated in this work. A comprehensive technological review with a strong focus on the challenge of producing physiologically relevant vascular structures is given. Finally, the remaining obstacles and opportunities in the development of vascularized Organ-on-a-Chip platforms for advancing drug development and predictive disease modelling are noted.


# 1. Introduction

In order to keep up with the medical promises of the 21st century regarding cost- and resource-efficient availability of drugs, predictive disease modelling and personalized medicine, there is an urgent need for powerful, highly reliable and physiological relevant in vitro tissue models. Up to now, comparably simple, two-dimensional cell cultures still represent the routine assays for the industrial screening of pharmaceutical substances[1]. Their popularity is primarily based on their low production and maintenance costs, established validation methods, and the possibility of fully automated, high-throughput screening[2]. However, despite their popularity, the current screening methods are prone to result in “late fails” in the drug development pipeline. These refer to drug candidates that appear promising in the first two development phases and only reveal serious side effects in clinical trials on patients[3,4]. According to expert estimates, the effective avoidance of these failures would lead to cost and time savings of up to 50 %[5].

To overcome these limitations and improve effectiveness in preclinical trials, research turned to three-dimensional cell cultures and scaffold based tissue models[6]. Amongst these, multicellular spheroids gained particular attention. Spheroid cultures have led to many discoveries with respect to cell behavior, drug efficiency and toxicity in the 2000’s due to their proximity in cell morphology[7–13]. In recent years, organoids as self-assembled 3D systems generated from progenitor cells have evolved as patient-specific, highly organ-mimicking systems for drug research[14,15]. These organ mimics stand out by enabling the inclusion of vasculature through incorporation of mesodermal progenitor cells[16] or by cultivation in a perfusion chip[17]. However, their limited size, complicated connection to a perfusion system and extensive sourcing of progenitor cells so far inhibits broader industrial application of organoids as vascularized organ models. Difficulties in targeted vascular perfusion also apply to 3D-scaffolds, in which perfusion with medium is generally possible. Still, these approaches cannot recreate the exchange and variation of chemicals, oxygen supply or mechanical stimulation, and make the detection of metabolic products difficult[18].

Recently, Organ-on-a-Chip (OOC) devices, which emerged in the last decade, experience a boost in combination with digitalized manufacturing processes such as bioprinting. They offer enormous potential to bridge the gap between scalable production desired by industry and the cell biological complexity required for efficient and predictive use. OOCs are microfluidic devices that cultivate an arrangement of cells under continuous perfusion to simulate tissue or organ physiology[19]. With these chips, metabolic products can easily be detected, drug administration efficiently executed and nutrient supply realized via a mimicked blood flow[20,21]. In the last ten years, major progress has been made in the speed and simplicity of the production process while increasing the complexity and physiological relevance of these devices[22,23]. Scalability, batch-production and high-throughput drug

screening platforms are still not advanced enough for standard application in clinical research though[24].

To create even more relevant OOC devices, it is important to include vascular networks into the devices to ensure oxygen and nutrient supply at distances greater than the nutrient diffusion length of 100 – 200 µm[25,26]. In the human body, a hierarchical network of arteries and capillaries ranging from diameters in the millimeter range down to 10 µm[27] exists. Endothelial lining of these vascular networks is extremely important to realistically mimic the uptake and distribution of nutrients or drugs, and hence to conduct physiologically relevant pharmacological or toxicological screening studies[28]. This becomes even more important for cancer studies and predictive disease modelling, as the biomolecule permeability, uptake of drugs, transport of secondary cell types and control of hydration levels are important therapy markers[29,30].

This paper will give a comprehensive overview of design approaches towards vascularized OOC devices. The versatility of production technologies, vascularization strategies, choice of materials and cell types will be summarized, depicted and critically discussed. To this date, a lack of a clear definition that outlines vascularized, three-dimensional OOC devices has hampered categorizing and crosscutting evaluation of these powerful bioengineering tools. In this article, we will therefore take a first step to illustrate, interpret and differentiate various OOC designs. Particular emphasis is given to those approaches that enable multicellular, spatially organized OOCs with open, perfusable and connected channel systems. These are categorized into biomimetic, biosynthetic, and self-assembled vascular structures and critically evaluated by their proximity to the anatomy and physiology of their native counterpart.

# 2. Cells and materials in Organs-on-a-Chip

As a first step in planning the production of an Organ-on-a-Chip, careful consideration has to be given to the selection of cell types and biomaterials suitable to mimic the desired tissue of interest. In particular, type, origin and spatial distribution of tissue specific stromal as well as parenchymal cells need to be analyzed. The following paragraphs elaborate on the cytological as well as ECM-related facets of OOCs with a primary focus on five exemplary organs (heart, lung, brain, liver, and kidney) that are of general interest in this field of research (Table 1).

According to Majno, three major groups of vascular endothelium can be found throughout the human body. The endothelium can exhibit a continuous cellular lining as present in muscle, brain and lung tissue, contain fenestrae like in the kidney, or have a discontinuous lining as found in the liver [31] (Table 1 and Figure 1). The shape and form of the microvascular network strongly depends on the specific organ domain and function. In the heart, the microvascular network is aligned with the myofibers[32], while it forms a spherical cluster in the kidney glomerulus for optimized waste product absorption[33,34]. At the same time, a high capillary number and density can be observed for both organs (Figure 1 A and D)[35]. In addition, differences in the cross-sectional morphology of capillaries are present. While the inner diameter of capillaries found in myocardium and the brain tissue is comparable[36], the thickness of cerebral capillary walls is 10-times higher and contains only very few membrane vesicles to form a tight blood-brain-barrier[37,38]. The unique endothelial composition correlates with its specific function in the organ, which can be oxygen or nutrient transfer, waste product uptake or release.

For the before mentioned reasons, reproducing the morphological and structural arrangement of the endothelium is of high relevance for the design of vascularized OOC. In addition, the thickness, composition and elastic modulus of the basal lamina, which differs for each organ, has to be

considered for the selection of an appropriate ECM-material that closely resembles the native environment.

## 2.1. Choice of Cells

Thoughtful cell type selection is of vital interest for the design of meaningful tissue models. The decision for and sourcing of primary cells, stem cells or established cell lines has been extensively discussed in previous review articles[32,39–41].

The selection of cells primarily depends on the specific biological question and on the parts or function of an organ that are to be studied. However, the choice of endothelial cells (ECs) influences the shape as well as structure of the resulting vascular network and should therefore be critically evaluated. For instance, Paek *et al*. could show that organ-specific ECs (e.g. adipose microvascular endothelial cells or retinal ECs) result in a denser and finer capillary network than when human umbilical vein endothelial cells (HUVEC) were cultured in the same environment[42]. Regardless of this aspect, over 70 % of the reviewed studies on vascularized OOCs turned towards HUVEC as a source of primary ECs. Their availability and their potential to spontaneously form vascular lumen structures in combination with other cells were the main reasons for their usage. Only in a few cases cell types that represent the tissue of interest's vasculature more closely, such as dermal microvascular ECs[43], liver sinusoidal ECs[44] or pulmonary microvascular ECs[45,46], were selected.

Apart from the EC source, the choice of co-culture cells greatly influences the shape and gene expression of the endothelium[47], which was presented in detail by Campisi *et al*. for the blood-brain-barrier. The morphology and connectivity of vascular networks between cultures of single ECs and co-cultures with brain astrocytes and pericytes strongly varied[48]. Fibroblasts and pericytes are stromal cells that affect microvascular network formation by secretion of growth factors and direct cell-cell interaction[49]. Half of the analyzed studies on vascularized OOCs use these as endothelial-stabilizing cells. Others co-cultured hMSC with endothelial cells, as they improve capillary formation by secreting vascular endothelial growth factor[50,51], exhibit the potential to differentiate towards smooth muscle cells (SMC)[52] and are reliably available.

An examples of a fully human, primary cell line based organ model was presented by Herland and co-workers with primary human hepatocytes in combination with liver sinusoidal microvascular ECs as a membrane liver model[44]. For a retina-blood barrier model, Paek *et al*. chose human induced pluripotent stem cell (hiPSC)-derived retinal epithelial cells in combination with primary sourced retinal ECs and fibroblasts[42]. HiPSC were also used by Campisi *et al.* for a blood-brain barrier model with primary human pericytes and astrocytes[48]. The examples above demonstrated that both the source of endothelial cells as well as the choice of surrounding stromal and parenchymal cells has a significant influence on the shape and function of the constructed endothelium. This influence becomes especially important if e.g. the nutrient uptake or the absorption of drugs or nanoparticles through the endothelium is the goal of research. Still, for studies on specific biological interfaces, isolated impact of a specific cell type or arrangement, or for proof-of-concept studies of an OOC-production method, this complex interaction may be less critical.

## 2.2. Materials for the cellular microenvironment and microfluidic chip design

In OOC devices, different material classes have to be selected for the extracellular matrix mimicking microenvironment and for the housing of the microfluidic chip. The choice of materials for the cellular microenvironment is very important for all OOC devices, as the interaction between cell and extracellular matrix (ECM) is crucial for organ function. The ECM provides cell adhesion ligands, is involved in the cells' response to biochemical signals and thus ultimately affects its phenotype[6]. Materials available for the cellular microenvironment in vascularized OOC devices include polymers

of synthetic origin, such as polyethylene glycol (PEG)[53,54], naturally derived hydrogels like agarose and collagen[55] as well as modified natural hydrogels like methacrylated gelatin (GelMA)[22,23].

Natural hydrogels often retain their biological activity, which is important for cell proliferation and differentiation. These materials offer arginine-glycine-aspartic-acid (RGD) amino acid sequences, which allow cell adhesion and proliferation by integrin-RGD binding[56]. This group of materials includes collagen and its derivatives gelatin and GelMA, fibrin and hyaluronic acid (HA)[23]. Other hydrogels such as alginate and agarose only allow cell encapsulation due to a lack of such motifs. They can, however, be turned into bioactive materials by adding amino acid sequences similar to RGD[57,58] or nanoparticle integration[59,60]. The same applies to PEG, which is a synthetic material and naturally not bioactive. The addition of RDG-motifs can provide bioactivity[61], or it can be added to other hydrogels like GelMA to increase the mechanical stability[52,62].

In an attempt to provide even more biomimetic cell culture environments, some groups turn towards decellularized ECM extracted from animals or human patients[63,64]. Decellularized ECM offers a natural and organ-specific environment, but requires intensive preparation and has to be acquired from an animal or via human biopsy. Its limited availability and batch-to-batch variation hinder the use of decellularized ECM for large scale assays. However, the ability of cells to produce their own ECM in cell culture can be utilized to overcome this limited availability by precultivation of cells on petri dishes, in well plates or on scaffolds[65]. Various cell types such as fibroblasts, MSC or cancer cells provide native ECM material that includes all vital components such as proteoglycans and fibrous proteins like collagen, elastin and fibronectin[66]. By choosing a suitable cell type or co-culture combination, the composition of the cell-derived ECM can be tailored to the tissue type of choice and e.g. promote osteoblast differentiation or vascular formation[67]. The drawbacks of sourcing the biomaterial from cell-cultures are the low productivity, inhomogeneity of ECM composition and intensive decellularization.

Besides its chemical composition, the materials' mechanobiological properties play a vital role in cell culture, too. For instance, it is well known that the elastic modulus of a hydrogel highly influences cell proliferation[68], differentiation of stem cells[69] as well as gene expression of differentiated cells[68]. Each type of organ has its own ECM composition and specific elastic modulus (Table 1), which changes with age[70] or illness[71–74]. The choice of material should aim for the appropriate stiffness, which is adjustable to a certain point by the degree of crosslinking as well as the concentration and composition of the chosen hydrogel. From a mechanical point of view, materials used for creating vascularized tissues are subject to partially conflicting requirements that are difficult to bring together. The necessity for a stiff and structural stable channel that withstands several weeks of dynamic culture opposes the need for a material exhibiting native vessel-like compliance[75]. When 3D-printing is employed, the list of conflicting demands is extended by the materials' rheology and printability[76,77]. Specifically designed blends of various hydrogels that balance stability, printability, stiffness and biological activity are a potential solution to this problem[78–80]. Balancing optimal material sourcing, bioactivity, cellular viability, differentiation and vessel formation with long-term mechanical stability under flow as well as good processability with the technology of choice is challenging and requires in-depth assessment.

Finally, the materials for the microfluidic chip embedding the organ tissue should also be taken into consideration. Polydimethylsiloxane (PDMS) for instance is a widely-used, albeit not optimally suited material for OOC applications. Soft-lithography based PDMS molding is frequently reported in microfluidics and extensively used in OOC devices, even though PDMS itself cannot be used in the organ part of the device. PDMS cannot incorporate cells[81], though it can be coated with hydrogels to allow for cell adhesion under perfusion[82]. Additionally, the mechanical and chemical nature of PDMS is not comparable to natural ECM and therefore does not mimic in vivo tissue. However, its

popularity has so far remained unaffected by these limitations due to numerous advantages, such as its transparency, high flexibility, easy fabrication and low price. Even more, the application of PDMS in quantitative OOC assays is questionable, as small hydrophobic molecules like drugs or fluorescent markers diffuse into PDMS and affect the accuracy of metabolic assessments[83,84]. Lipophilic coating of PDMS[85], plasma treatment[86] or saturation of the PDMS surface with phospholipid polymers[87] can prevent unintended protein uptake. Other materials such as polystyrene (PS) and PMMA show lower small protein absorption than PDMS, but also lower gas permeability and are difficult to process[85,88,89]. Borosilicate glass is the gold-standard in cell culture, because of its superior microscopic properties and high biocompatibility. Moreover, it exhibits a very low small molecule absorption and improved cell adhesion compared to PDMS. However, its challenging processing and the restricted geometrical complexity that can be achieved prevents the production of fully glass based OOCs[90]. Recently, materials that not only exhibit a low small molecule absorption, but are also 3D-printable, have gained particular attention. They not only reduce unintended protein uptake, but also enable parallel printing of the chip itself and organ mimicking bioinks in a single process. For example, Lee and colleagues printed a PCL-based microfluidic chip that contained the bioprinted tissue sample. The chip exhibited a lower protein absorption than PDMS, but it also lacked transparency[91].

In conclusion, the ideal material for the production of Organ-on-a-Chip devices that offers transparency, biocompatibility, low side effects on quantitative assays as well as good processability is still not available and its discovery merits further investigation.

*Table 1: Selection of exemplary organs with their cellular components, vascular structure and characteristics, basal lamina components and elasticity.*

| | **Heart** | **Lung** | **Brain** | **Liver** | **Kidney** |
|---|---|---|---|---|---|
| Exemplary organ component | Myocardium | Alveolus | Blood-brain-barrier | Hepatic lobule | Glomerulus |
| Type of endothelial lining[31] | Continuous | Continuous | Continuous | Fenestrated | Discontinuous |
| Parenchymal and stromal cellular components | Coronary ECs<br>Pericytes<br>Coronary fibroblasts<br>Cardiomyocytes[92] | Pulmonary ECs<br>Alveolar type I cells<br>Alveolar type II cells[93] | Cerebral ECs<br>Pericytes<br>Astrocytes[37] | Liver sinusoidal ECs<br>Hepatocytes<br>Stellate cells<br>Dendrite cells[36] | Glomerular ECs<br>Glomerular mesangial cells<br>Podocytes<br>Epithelial cells[94] |
| Capillary structure | Dense capillary network with 8 µm average diameter, alignment along myofibers[33,92] | Branched capillary network with many membrane vesicles for oxygen transport[38] | Very tight and thick endothelium, small capillaries of 7-10 µm with few membrane vesicles[37,38] | Highly perforated sinusoid of 10-40 µm diameter with gaps of 100-200 nm in between[47,95] | Dense network of perforated capillaries with fenestrae of 60-80 nm in spherical cluster arrangement[34,94] |
| Basal lamina | Mainly collagen I and III [92] | Very thin (100 nm) with mainly collagen I[96] | Very thin (20-100nm)[38] with mainly collagen IV and laminin[97] | No lamina in sinusoids, only some in space of Disse [95] | Mainly collagen IV[34] |
| Elastic modulus healthy tissue | 2 – 8 kPa[98] | 2 – 5 kPa[96], increases with age[70] | ~3 kPa[71] | 1 – 3 kPa[72] | 2 – 4 kPa[34] |
| Elastic modulus diseased tissue | Increases with cardiac hypertrophy[73] | Increases with fibrosis to up to 16 kPa[74] | Reduced by Alzheimer's disease to 2 kPa[71] | 2-4 old increase with fibrosis caused by hepatitis[72] | Reduced by half by renal ischemia[34], increased with fibrosis[74] |

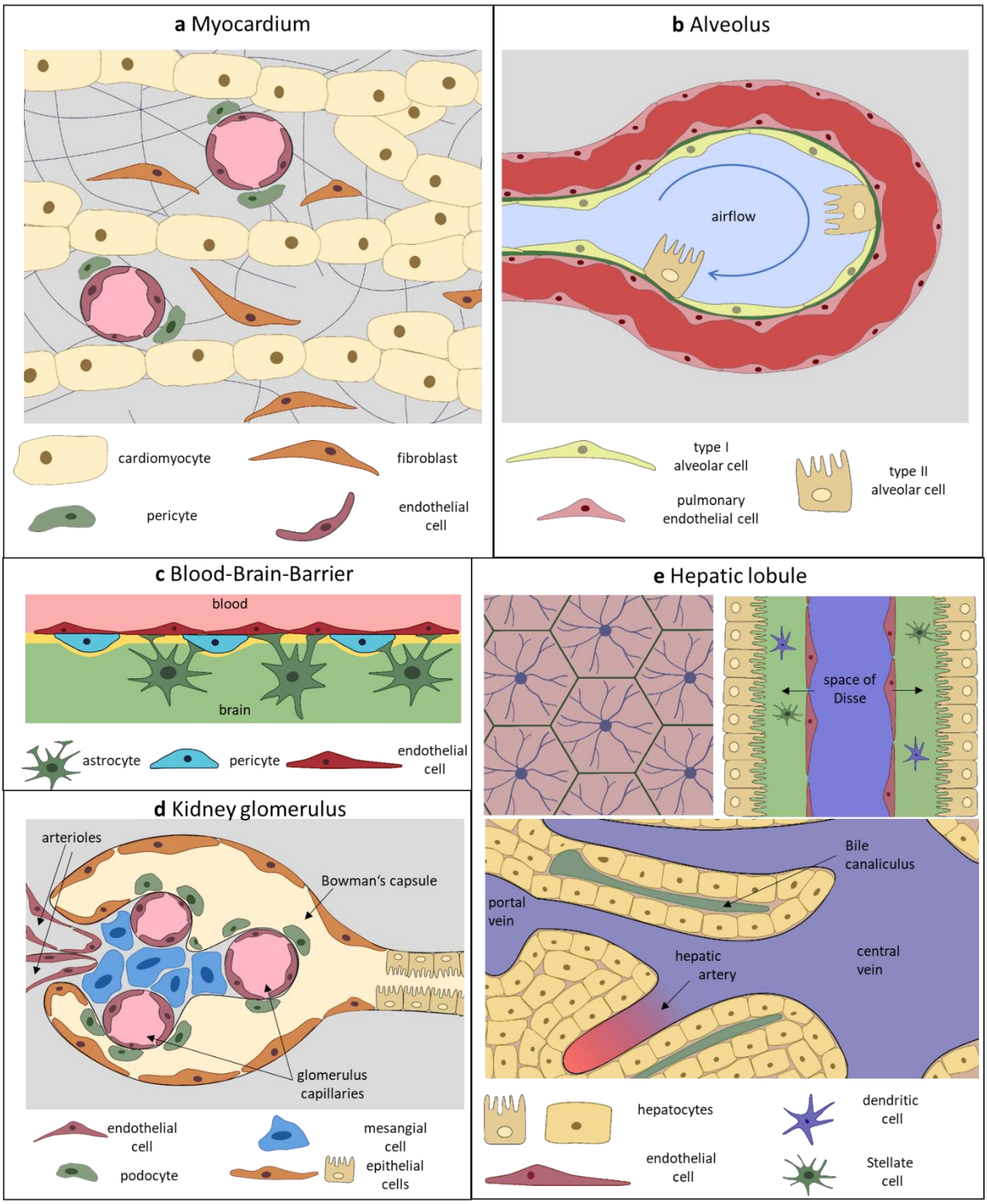


*Figure 1: Structural and cellular representation of myocardium (**a**), alveolus (**b**), blood-brain-barrier (**c**), kidney glomerulus (**d**) and hepatic lobule (**e**). Figures inspired by following publications for the myocardium[92] (a), alveoli (b)[45,96], blood-brain-barrier[37](c), glomerulus[34,99] (d) and hepatic lobule[95] (e).*

# 3. Fabrication of vascularized Organs-on-a-Chip

Organs-on-a-Chip are not only applied during drug development as platforms for drug toxicity screening[100], studies on the impact of nanoparticles[101] or monitoring of pharmacokinetics and pharmacodynamics[44], but also in fundamental research on angiogenesis[102], tumor growth and spreading[103] as well as on barrier function and permeability[45,104]. As versatile as these applications are the fabrication strategies for OOCs, which will be presented and discussed in this section.

Vascularized OOCs can be classified regarding production, structure and material selection into the three categories biosynthetic, biomimetic and self-assembled, which are distinguished presented and discussed hereafter. According to existing classifications of biomaterials[54,55], biosynthetic OOCs are defined as devices that spatially organize cells with synthetic materials, which remain within the tissue during cultivation and therefore do not exactly reproduce the biological tissue composition[54]. They typically include a layer, compartment or membrane of synthetic material that partially separates the cells in the area under investigation. In contrast, biomimetic OOCs try to recapitulate the native morphology and vascular tissue structure as close as possible with modern fabrication technologies[55]. They mostly include natural hydrogels as basis for the cellular microenvironment to allow cellular proliferation in three dimensions and add biological and mechanical cues similar to the in vivo condition. The vascular structures within these cellular arrangements are generated in various sizes and shapes depending on the selected biofabrication technique[52,105]. OOCs that utilize the capability of endothelial cells to create intricate vascular networks de novo via angiogenesis or vasculogenesis are denoted as self-assembled[42,106] or self-ordered[48] vascular networks in literature, and are defined as self-assembled microvascular networks in this work.

## 3.1. Biosynthetic OOC devices

In general, biosynthetic fabrication approaches apply synthetic elements to support the fabrication of spatially organized tissue mimics, which can be cultured and investigated under native perfusion conditions. The synthetic material is used to structure, compartmentalize, and separate cells with different functions. Despite their geometrical partition, incorporation of pores or gaps in the compartment walls allows direct cell-cell-interaction. Examples of biosynthetic approaches include membrane-based devices, channel structures and polymer sheet stamping. These devices involve synthetic materials to structure, compartmentalize and separate cells, with pores or gaps in the compartment walls that allow cell-cell-interaction.

### 3.1.1. Membrane-based OOCs

Membrane-based OOCs are PDMS-based microfluidic devices with channels separated by thin porous membranes, which are fabricated by soft lithography and molding. These systems have been extensively used in the past to study the influence of mechanical stimulation or deformation on the lung[107], kidney glomerulus[108] or the influence of cancer drugs on renal tubules[109] with various porous membrane materials (Figure 2a). The group of Donald Ingber has further developed this approach and used a porous, ECM-coated PDMS-membrane system for various organs like the lung[45,110], gut[111,112] and bone-marrow[113] that can include mechanical stimulation. They even achieved complete Body-on-a-Chip systems by coupling various OOCs on a specially designed platform[44,114]. Each Organ-on-a-Chip consisted of a square microfluidic channel (400 x 100 µm) separated by a membrane with 10 µm small pores lined on the vascular side by endothelial cells and by tissue-specific cells on the parenchymal side. Using a robotic pipetting system, medium could be transferred between the organ containing wells, or withdrawn for individual drug conversion and metabolic product analysis[114]. In these models, cells exhibited tight intercellular junctions through the gaps in the membrane, which was successfully employed to model the drug uptake and metabolic response of the organs[44]. It also demonstrated that Bodies-on-Chips could accurately predict the metabolic conversion of drugs,

indicating that the smart combination of OOC devices can greatly improve the significance of toxicity studies in pharmaceutical research[44].

### 3.1.2. Parallel channel based OOCs

Parallel channel OOC systems are based on a microfluidic chip that is sectioned into various parallel channels, which are connected via small gaps in the channel wall. Two perfusable channels, a vascular endothelial cell lined channel and a channel for the inlet of organ-specific medium, are the basis for these OOCs. These devices are similar to membrane-based approaches regarding the synthetic barrier formed between different cell types. However, in contrast to the membrane design the cells are not only seeded two-dimensionally, but can be cultured in a 3D-microenvironment. For this purpose, one or more hydrogel-filled compartments representing the parenchymal space are located between the two channels. The small gaps in the compartment walls enable a direct cell contact and can be used to monitor cell interactions, vascular formation and cancer cell invasion.

Recently, studies on the invasion of breast cancer cells into bone tissue[115], on stromal cancer invasion[116] and on the influence of cancer cells on the endothelial barrier function[117] have successfully been conducted using parallel channel OOCs. Adriani and colleagues could show that the choice of ECs in a blood-brain-barrier model with rat neurons and astrocytes cultured in collagen influences the permeability of the barrier. Cerebral microvascular ECs showed lower dextran permeability than HUVECs and formed a tight barrier against the neurotransmitter glutamate[104] (Figure 2b).

### 3.1.3. Polymer sheet stamping for OOCs

Zhang *et al.* presented a specially developed, biodegradable and mechanically tunable polymer (POMaC) as an alternative to PDMS in OOCs. In their work, POMaC sheets were UV-patterned on a master mold and stamped to form a chip containing a network of channels, cavities and micro-pores ranging in sizes of millimeter down to 10 µm[118]. The stamped sheets are transferred into a microfluidic chip and the channel insides are coated with gelatin, which allowed the seeded HUVEC to form a tight endothelial lining. Embryonic SC derived hepatocytes or cardiomyocytes with hMSC as support cells were casted in Matrigel in the parenchymal space to create sophisticated Livers- and Hearts-on-a-Chip. They also studied the conversion of the antihistamine terfernadine and how the addition of thymosin promoted angiogenesis through the micro-pores into the surrounding hepatocyte space (Figure 2c). This platform was further advanced by Lai *et al.* using a slightly modified polymer and a single straight channel to fit into a 96-well plate array[119]. They included carbon electrodes for the electrical stimulation of hiPSC-derived cardiomyocytes and measured the contraction with integrated microcantilevers. With a further developed Body-on-a-Chip device, they could demonstrate an increased tumor toxicity of the cancer drug Tegafur by coupling a liver and a breast cancer tissue chamber. Even more, cancer cell invasion into the liver tissue through the fabricated vasculature could be detected.

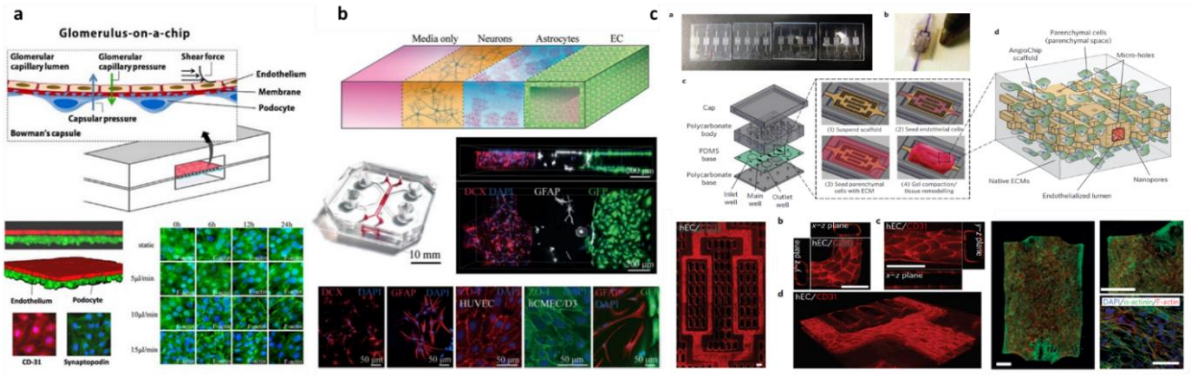


*Figure 2: A membrane-based Glomerulus-on-a-Chip with endothelial cells and podocytes[108] (**a**), parallel PDMS channels of endothelial cells, astrocytes and neurons as a blood-brain-barrier chip[104] (**b**) and PoMAC sheet pattering and stamping for a Heart-on-a-Chip as well as a Liver-on-a-Chip[118] (**c**).*

### 3.1.4. Comparison and summary of biosynthetic OOCs

Among the described biosynthetic OOC fabrication methods specific difference can be observed. In polymer sheet stamping and parallel channel based OOCs cells can be cultured within a three-dimensional environment. In contrast, membrane-based approaches provide a rather planar cell seeding surface. Even though the planar culture does not recapitulate native tissue, it allows controlled cellular positioning and thereby facilitates microscopy and immunostaining analysis. The nutrient supply strategy also differs among the presented methods. In all channel and most membrane-based devices, cell-specific medium is supplied through the parenchymal channel side and not through the endothelium-lined channel. This offers practical cell culture advantages, but at the same time provides a less biomimetic environment. For instance, cell-specific medium can be easily administered, therefore avoiding possible conflicts in different nutrient preferences of included cell types. However, the medium directly reaches the cells without passing the endothelial barrier, which would naturally control the permeability of drugs, small molecules, respiratory gases, and nutrients.

In biosynthetic fabrication approaches, the chips are generally fabricated by lithographic techniques, which offer a great freedom concerning the complexity and size of the fabricated structures. So far, the presented works on parallel channels and membrane-based devices mostly integrate channels with sizes in the range of arterioles, ranging from 120 µm to a millimeter in width at heights of around 100 – 200 µm. The high resolution of the lithography processes, which could principally be used to produce capillary vessels, indicates the promising future potential of biosynthetic approaches and gives reason to expect further exciting studies in this area.

Despite their differences, all presented biosynthetic fabrication approaches have in common that a synthetic material is used to partially separate different co-cultivated cell types in the area under investigation. A limited but precisely controllable contact area is given either through the pores of a membrane or through gaps in the channel wall enabling direct cell-cell-contact and cell-cell-signaling. Potential drawbacks or side effects of the localized and limited contact area, such as localized drug uptake, undesired mechanical or biological cues caused by the elevated material stiffness, or general lack of an uninterrupted endothelial interface have not been reported yet, and merit further investigation. On the other hand, biosynthetic approaches offer a great control over cell distribution and can provide specifically tailored material as well as medium properties for every cell type. Even more easy coupling to complex perfusion systems was shown for Bodies-on-a-Chip[44], cell-cell interaction studies[104], and monitoring of cancer invasion[116].

A detailed overview over the presented works based on biosynthetic approaches is given in Table 2 at the end of this review.

## 3.2. Biomimetic vascular structures

Biomimetic production approaches try to mimic both the vascular anatomy and physiology of native tissue and often incorporate natural hydrogels as bioactive materials. An important feature that distinguishes biomimetic from biosynthetic models presented before is that no synthetic material separating the cells is left in the vascularized area after production. Fabrication approaches of open, perfusable channels in a hydrogel matrix are highly versatile, ranging in size and shapes from a few micrometers to millimeters and can be round or rectangular.

### 3.2.1. PDMS stamping

Early works on vascularized hydrogels use traditional soft lithography processes to create a PDMS stamp. This stamp can either be directly casted in a hydrogel such as agarose[120,121] or act as a master mold for a sacrificial gel like gelatin first[43,122]. A typical example are Golden and Tien, who used classical soft lithography to create a very fine hexagonal mesh with microchannel sizes down to 6 µm. Their device supported endothelial growth and perfusion inside the channels with dermal fibroblasts in a hydrogel of choice casted around the channel network[43]. An innovative method was presented by He *et al.*, who exploited naturally occurring fine hierarchical networks by copying the leaf venation of a mulberry leaf in agarose to create a simple liver model with HUVEC inside the channels and HepG2 cells in agarose [121]. This model was further improved by the same group to feed hydrogel-cell mixtures in PDMS-casted microwells via a PDMS cast of the leaf venation[123]. By scanning the leaf, a complex CAD-model was generated as an enhancement of the process, since the digital model enables precise placement of the 2 mm wide microwells for optimal nutrient supply[124]. The PDMS-casted device was used as a Body-on-a-Chip platform with a HepG2-HUVEC cell mixture in fibrin as liver tissue and a hMSC-HUVEC mixture as bone tissue to study the invasion of pancreatic cancer cells (Figure 3a). The inclusion of HUVEC in the tissue led to the formation of open lumen structures inside the chambers and with that to an enhanced nutrient and oxygen delivery inside the chambers.

### 3.2.2. Hydrogel casting

Hydrogel casting around structures is a very common method and is employed in other approaches as well. Simple channel systems can be formed by placing one or multiple needles or rods inside a microfluidic chip and casting a hydrogel of choice around[125]. With coaxial needles, Hasan *et al.* fully reproduced the arterial structure with HUVEC, fibroblasts and smooth muscle cells in GelMA (Figure 3b)[126]. Since casting of rods or needles is limited in geometry and number, they were replaced with the emergence of 3D printing by extrusion printed fibers. Just as before, the printed fibers with a diameter of down to 100 µm are first embedded in a hydrogel and pulled out afterwards. Connecting these tissues to a pump system leads to perfused OOCs. This method has been used to create vascular networks in a cast of various hydrogels containing pre-osteoblasts[127] or liver cells[128], with the inside of the channels lined with HUVEC (Figure 3c). In contrast to needle casting, the channel network can be printed in regular or even chaotic ways and the cross-sectional size can be tailored by the nozzle diameter. The drawback remains that the fibers have to be removed manually later on, hindering the creation of more complex structures and vascular networks.

To generate even more biomimetic, vascularized Organs-on-a-Chip, 3D-bioprinting technology recently gained particular attention[77,129]. Instead of solely 3D-printing the vessel template, it allows parallel printing of vessels, voids, ducts and multiple spatially organized cell types. It is therefore considered as a key technology for the production of biomimetic tissues and vascularized OOCs. Various production strategies using 3D-bioprinting exist for OOC-devices, such as direct[130] and sacrificial[63] 3D-bioprinting or coaxial nozzle extrusion[52,62].

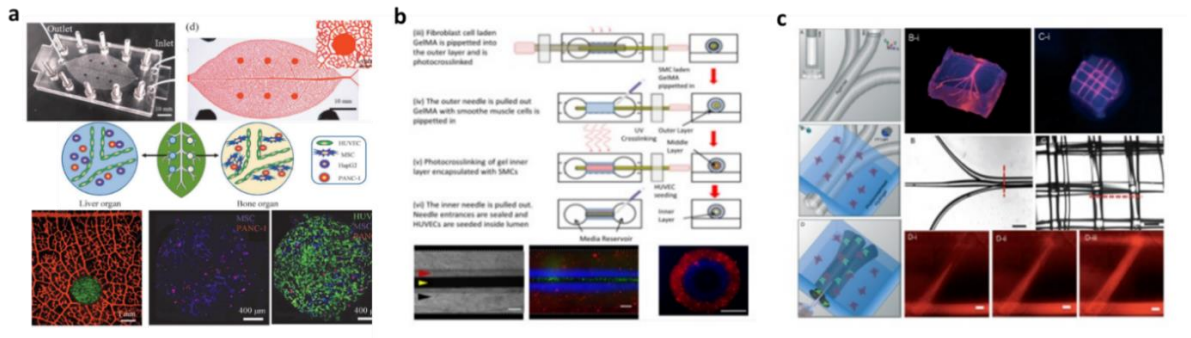


*Figure 3: Various production techniques that require casting of a master mold in an ECM material. Examples contain the copy of a plant leaf venation in PDMS to create vascular networks that support liver and bone tissue in fibrin[124] (**a**), coaxial nozzle casting in GelMA for a complete artery structure with HUVEC, fibroblasts and SMC[126] (**b**), and 3D-printed agarose fibers casted in a hydrogel of choice and lined with HUVEC[127] (**c**).*

### 3.2.3. 3D-bioprinting with sacrificial materials

The use of sacrificial materials is a common technique to create open and perfusable channel structures. Vessel structures are often 3D-bioprinted with a sacrificial material, which is afterwards removed thermally or chemically. The surrounding, stable ECM materials are either casted around the printed structure or directly printed as well. The most common sacrificial materials are gelatin, as it dissolves at cell culture temperatures, and Pluronic F 127, which liquefies when cooled below 4°C. Several advantages of extrusion or drop-based 3D-bioprinting with sacrificial materials over soft lithography or stereolithography (SL) printing exist. These include the simple implementation of multi-material printing, the lack of potentially toxic cross-linkers when using natural hydrogels, and the shape of the formed vessels, which are truly round and mimic the native vessel shape. Complex, branching, and three-dimensional networks are the result of this print process and do not require manual removal steps.

For any production technique, many research groups turn to gelatin as sacrificial material[63]. Using gelatin in combination with extrusion printing, Lee and Cho fabricated a very straightforward Liver-on-a-Chip. They chose a simple design with a single 400 µm wide, 15 mm long straight channel lined with HUVEC and HepG2 casted in a collagen matrix[91]. The design itself is very plain, yet the housing is highly notable, as it was printed with PCL on glass instead of produced by PDMS molding. A comparison of the albumin and urea secretion of cells cultured in the PCL chip with those in a fully PDMS-based chip showed that PCL has much lower protein absorption. This highlights that the choice of chip material has a significant influence on the outcome of gene expression assays in OOCs.

Schöneberg *et al.* also employed gelatin as a sacrificial core material with HUVEC and a surrounding fibrin layer with SMC, which they multilayer-printed with a microvalve drop-on-demand printer. Fibroblasts in a collagen gel were then cast around the printed vasculature to fully recreate a perfusable three-layer artery model[27]. In a similar approach, Campos and co-workers created a vascularized model of the neural stem cell niche. iPSC derived neural progenitor cells were printed together with HUVEC-coated vasculature and dynamically cultured in a perfusable microfluidic chip (Figure 4a)[131].

The group of Jennifer Lewis has developed an extrusion-based printing platform with Pluronic F 127 as sacrificial material that has been successfully used over the years. Kolesky *et al.* showed in 2016 that centimeter-thick printed and vascularized tissue models remain viable for over 6 weeks[132,133]. The sacrificial vessel network as well as an hMSC-containing gelatin-fibrin network were extrusion printed and casted in a gelatin-fibrin matrix containing hNDF. Seeding of endothelial cells inside the 600 µm large channels after thermal removal of Pluronic led to the formation of a tight endothelial lining with good barrier functions. The same platform was used by Homan *et al.* to print perfusable

renal proximal tubules formed by proximal tubule epithelial cells. The centimeter long tubules were housed in a gelatin-fibrin matrix with rat fibroblasts as stromal cells. Culture under perfusion for over two months led to a tight epithelial layer and the cells reacted to the nephrotoxin Cyclosporine A[134]. This model was modified by Lin *et al.,* who added a vascular channel lined by glomerular microvascular endothelial cells next to the tubule channel[135]. A study on the albumin uptake and glucose reabsorption was successfully conducted and the cross talk of the proximal tubule epithelial cells with the endothelium during hyperglycemia monitored (Figure 4b).

Miller and co-workers chose a very different material for their Liver-on-a-Chip containing HUVEC and primary rat hepatocytes. They developed a carbohydrate-dextran glass material that can be embedded in any type of ECM material containing the parenchymal cell type of choice. The glass shows a good stability after printing and can form complex structures with vessel diameters of around 100 µm (Figure 4c)[136]. This is the smallest vessel diameter of any extrusion or drop-based printing approach observed in our study. It demonstrates the importance of tailoring material properties to the selected bioprinting process in order to fully exploit its capabilities.

### 3.2.4. 3D-stereolithography bioprinting

Stereolithography was the first 3D-printing technique invented, but its use in bioprinting is limited due to the photoinitiators, the comparably large ink volume needed and that for a long time only one material could be used at a time. Recent advances have made the sequential input of various inks possible[130], but the process is still time-consuming and requires manual work. Nevertheless, stereolithography is an appealing technique as it offers a much higher resolution than other 3D-printing technologies and does not require sacrificial materials for the fabrication of open channels.

One of the first groups to sequentially print various cell inks in a DLP based printer were Ma *et al.* in 2016, who used stem cell laden GelMa and hyaluronic acid to print complex hexagonal liver lobules[130]. Zhu and co-workers used the same technique and materials, but demonstrated that their vascular network could be made perfusable by adding hyaluronidase, which degraded the GelMA-HA ink. Their liver model consisted of HepG2 cells with mouse fibroblasts as perivascular cells around a HUVEC network, but it was implanted and assessed in vivo instead of being used as OOC[137]. They also improved the resolution of the print process compared to Ma's work and printed a network mimicking the rat capillary network ranging in size from 5 to 50 µm, proving the exceptional resolution of stereolithography printing (Figure 4d).

Grigoyan *et al.* presented that open vascular networks could be directly printed in PEG-DA[138]. They printed a full lung model with a 250 µm wide, perfusable vascular network around empty alveolar air ducts. They encapsulated human lung fibroblasts in the bulk hydrogel and lined the alveolar ducts with alveolar epithelial cells. Although no endothelial lining of vessels was included in their Lung-on-a-Chip, perfusion with blood, cyclic ventilation and monitoring of oxygen transfer between blood and alveolar channels was shown to be possible. The same group also printed a Liver-on-a-Chip by placing rat hepatocyte aggregates in a fibrin gel chamber and seeding their vascular channels with HUVEC (Figure 4e).

### 3.2.5. Comparison and summary of biomimetic OOCs

The overview of possible biomimetic fabrication strategies highlights the diversity and flexibility of available methods. Classic fabrication methods such as soft lithography and molding offer the highest resolution of all presented technologies, with minimum vessel sizes in the range of native capillaries. However, the production of the master mold is time consuming and requires expensive machinery. Multilayered, 3D vascular structures can only be achieved by manual stacking of multiple single layers. Instead, 3D-bioprinting offers the possibility to create branched and intricate vessel networks covering various length scales, and multi-material, 3D-architectures can be fabricated in a short time.

Open channels for vascular networks or for air ventilation can be simply designed. With sacrificial materials, channels with round cross-sections that mimic the native vessel shape can be formed. However, the resolution of channels generated by direct bioprinting is so far limited to approximately 100 µm. In addition, large-scale networks struggle with the required mechanical rigidity during fabrication, which requires careful tailoring of the bioink. Furthermore, 3D-bioprinting can generate multi-layered vessels that reproduce the complex cellular architecture of arterioles or arteries with smooth muscle cells and fibroblasts surrounding the endothelium. This has been demonstrated with drop-based[27,139,140] and coaxial nozzle extrusion[52,62] bioprinting. Multi-layer fabrication is complex, time-consuming and still limited to diameters of over 400 µm, which so far prevented it from being incorporated into vascularized OOCs.

A general advantage of biomimetic fabrication is the absence of synthetic material in the cellular microenvironment, enabling direct cell-cell contact between vasculature and surrounding parenchymal and stromal cells. The drawbacks include the low productivity, elaborate manual work and limited reproducibility, as well as reduced control over the cellular arrangement and over immunohistological assays.

A detailed overview over the presented works based on biomimetic approaches is given in Table 3 at the end of this review.

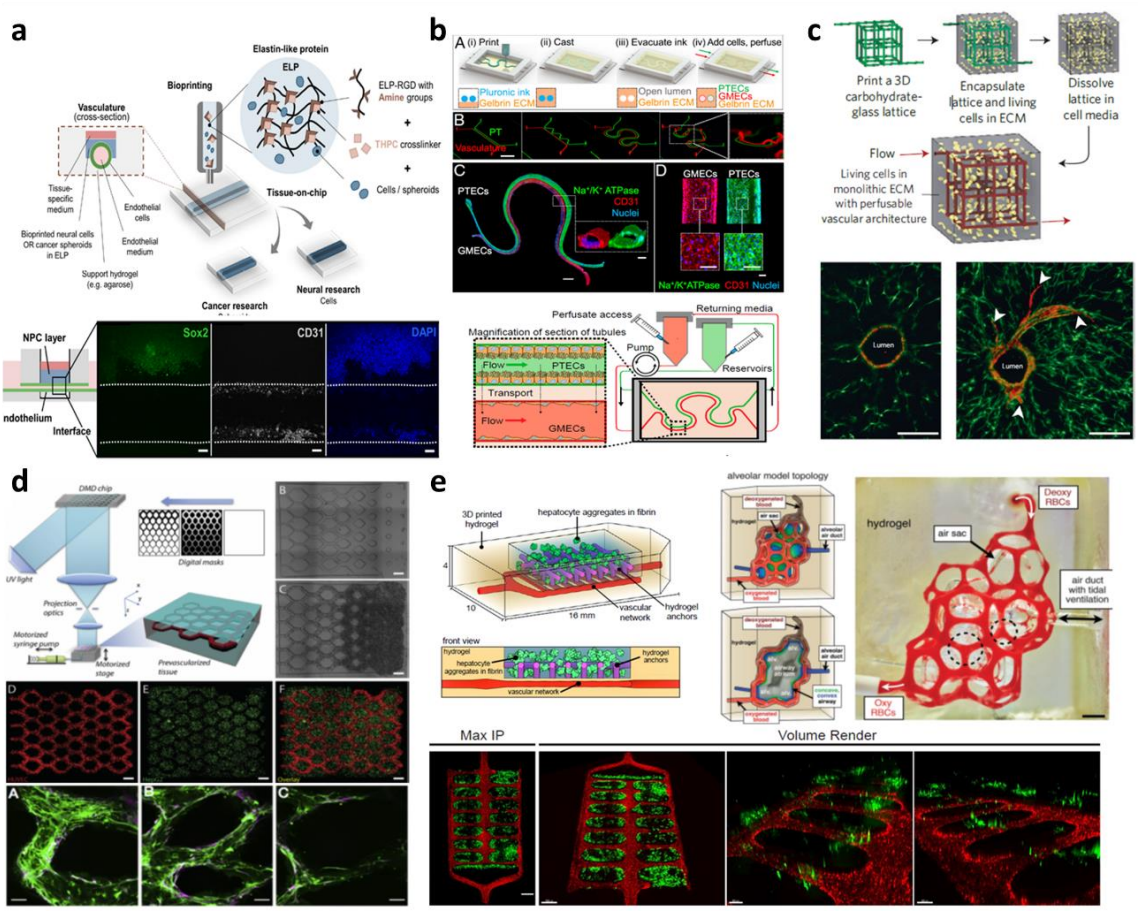


*Figure 4: 3D-printing of sacrificial materials such as gelatin using a DoD printer[131](**a**), extrusion printed Pluronic F-127[135] (**b**) or carbohydrate-glass[136] casted in ECM materials (**c**). Stereolithographic printing of hepatic tissue[141](**d**) and kidney or inflatable lung analogues containing various alveoli structures[138] (**e**).*

## 3.3. Self-assembled microvascular networks

Endothelial cells seeded in a hydrogel matrix can form intricate microvascular networks on their own. This capability for self-assembly of vascular networks has two possible origins. The first one, vasculogenesis, refers to a complete new formation of vascular structures by endothelial progenitor cells, while the process of capillary sprouting from existing blood vessels is called angiogenesis[26]. An anastomosis describes the connection of these new vascular networks to a larger, pre-existing blood vessel[142].

These self-assembled microvascular networks can be utilized to incorporate small vessel networks in OOCs. This is most commonly done by culturing endothelial cells in a hydrogel matrix between larger, perfused channels that mimic arterial and venous flow. Interestingly, these medium feeding channels are mostly generated based on biosynthetic or biomimetic fabrication strategies, including parallel channels[143], injection-molded devices[103], membrane-separated sections[42] or round channels that are 3D-bioprinted with sacrificial gelatin[139,140,144,145]. The pre-fabricated channels can be the source of endothelial cells for angiogenesis, or can be connected to the self-assembled vascular networks via anastomosis for targeted perfusion of the networks.

In the past years, self-assembly platforms to study angiogenesis or vasculogenesis have been extensively investigated. Researchers have studied the vascular formation of HUVEC in dependence of co-cultured cells[146,147], flow rates[148–150] or supplied growth factors[151]. Aside from fibrin and collagen, angiogenesis is also possible in RGD-modified PEG[106], GelMA[152] and thymosin β4-hydrogel[153]. The size of the created blood-vessels can also be tailored by the device architecture, as was shown by Yeon *et al*., who guided the angiogenesis to the desired vessel size with a PDMS ladder structure[154].

### 3.3.1. Microvascular self-assembly in parallel channel devices

A device set-up with parallel channels is a common choice and has been employed by Bang *et al.* for a blood-brain-barrier model with HUVEC, lung fibroblasts and rat astrocytes[143]. Campisi *et al.* chose the same device design, but they presented a fully human blood-brain-barrier model with primary pericytes and astrocytes as well as hiPSC-derived ECs[48] (Figure 5a). Their Brain-on-a-Chip exhibited a smaller vessel diameter of around 20 µm, higher capillary network complexity, higher protein expression and lower dextran permeability when ECs were cultured with astrocytes and pericytes instead of only pericytes. These characteristics come close to the in vivo BBB regarding vessel size, permeability and basal lamina composition (Figure 1 and Table 1).

A similar device setup with diamond-shaped chambers lined by 100 x 100 µm channels was presented by the group of Christopher Hughes[148]. In this device, angiogenesis and anastomosis of endothelial colony-forming cell-derived ECs in co-culture with lung fibroblasts was completed after 5 - 7 days of culture, with a natively formed basal lamina comprising collagen I and IV[155]. For a Cancer-on-a-Chip model, they cultured six different cancer cell lines together with ECs and fibroblasts in a fibrin gel. The cancer cells spontaneously formed spheroids that were connected to the microvascular networks. They observed differences in growth rate, vessel formation and collagen deposition for each tumor type and detected varying responses to various FDA-approved anti-cancer drugs. Phan *et al.* further developed this platform to fit into a 96-well plate and also observed a stronger reaction of colorectal cancer cells in 3D- and tri-culture to these anti-cancer drugs compared to mono- or 2D-culture[156]. This device can be combined with standard well plates, requires only small volumes of media and is driven by hydrostatic pressure. Additionally, endothelial lining of the channels reduces unspecific absorbance of the underlying PDMS. Their system could accurately predict tumor reaction to drugs, included the connection of the self-assembled tumors to a vascular network and exhibited basal lamina production (Figure 5b).

### 3.3.2. Radially oriented microvascular self-assembly

The group around Noo Li Jeon avoided the use of PDMS due to its previously described challenges regarding scalability and small molecule absorption[84]. Instead, they injection-molded circular devices in polystyrene on pressure-sensitive adhesive coated polycarbonate[157] that could be placed into 96-well-plates[158]. By filling the devices with fibrin gel and either lung fibroblasts or HUVEC, vascularization and dose-dependent response to angiogenetic inhibitors could be monitored [157,158] (Figure 5c). The addition of spacing between the chambers was employed for a versatile BBB-model. Human brain microvascular ECs and fibroblasts were co-cultured on one side of the channel and formed vessel networks reaching into the central chamber, where they connected to human astrocytes[159]. The same group modified the platform to house a 500 µm large glioblastoma tumor spheroid in its center. HUVECs showed a changed morphology and angiogenic sprouting in presence of the tumor compared to a single co-culture with fibroblasts[103]. This result underlines the great influence of parenchymal cells on the vasculature morphology and function. The device could be a suitable platform for the pharmaceutical industry as injection molding based fabrication processes can be easily scaled up. The small size, resulting in fast vascularization within only 4 days, and the combination with standard microplates are additional benefits, though perfusion of the device has yet to be incorporated.

### 3.3.3. Combined vascularization approaches

Two groups have presented an OOC where self-assembly approaches are combined with biosynthetic interfaces. Here, a parallel channel setup forms the basis for the generation of self-assembled vascular networks. These networks are later combined with a membrane-based interface over an open-top setup, where parenchymal cells can be placed on top to model cellular barriers or interfaces. Paek *et al.* presented a device made of PDMS with a hydrogel-cell mix containing fibrin, HUVEC and lung fibroblasts between 400 µm wide microfluidic channels[42]. The cells formed a tight vessel network with diameters of 10 – 25 µm and underwent anastomosis to the inlet channels in 7 days. The open-top design allowed the study the retinal pigment epithelium and microvasculature interface. HiPSC derived retinal epithelial cells (RPE) interfaced with organ-specific primary retinal microvascular ECs and choroidal fibroblasts in a specifically tailored fibrin-collagen I hydrogel exhibited a 50 % increase in specific basal lamina production and a 2.5-fold increase in pigmentation in contact with the capillary network. The culture of an adipose-tissue model based on human adipose derived SC and primary microvascular ECs was possible for 49 days, which was enabled through a functional vascular network, providing long-term nutrient and oxygen supply. This work also underlined the importance of ECs in stem cell differentiation as well as their role in determining size and structure of the formed vascular network. Even more, the integration of a lung tumor spheroid to the vascular network was also possible and resulted in an increased reaction to anti-cancer drugs (Figure 5d).

While most researchers use PDMS soft lithography to produce their chip, Park *et al.* 3D-printed parts of the microfluidic chip with PLA for a Lung-on-a-Chip model[147]. The tissue model itself was bioprinted with microvascular ECs and lung fibroblasts in a tracheal mucosa dECM material. Besides its innate suitability as mucosa model material, the ECM exhibited positive angiogenic effects. Finally, human tracheal epithelial cells were cultured in a transwell insert and placed on top of the vessel network. The contact area between epithelium and vascular network increased the epithelium differentiation, showed significantly higher transepithelial electrical resistance comparable to human donors, and a strong mucus reaction to the addition of interleukin 13 as an asthmatic inducer.

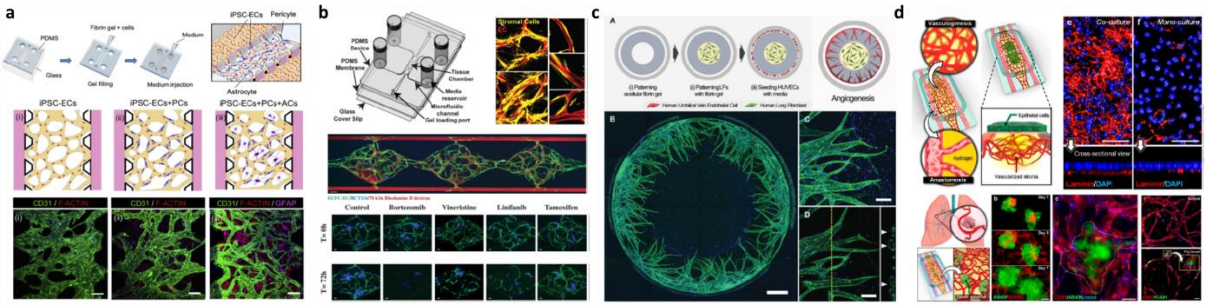


*Figure 5: Vascular formation in a hydrogel matrix in a device based on a parallel chip geometry for a blood-brain-barrier model[48](**a**) or Cancer-on-a-Chip [155,156] (**b**), in an injection molded PS chip for ocular angiogenesis[157] (**c**) and as a combination of parallel channels and membrane on top for a Retina- and Cancer-on-a-Chip[42] (**d**).*

### 3.3.4. Comparison and summary of self-assembled microvascular networks

The presented works prove the importance of vasculature on the function of any type of parenchyma, that the type of endothelial cell determines the characteristics of the vascular network and that the existence of such a network influences gene expression and cellular proliferation. By preparing larger channels and inducing de novo vascular formation, multiple scales and morphologies of vasculature can be achieved naturally only through dynamic interactions of endothelial cells with the ECM, pro-angiogenic factors, co-cultured cells as well as applied fluid flow[149]. The capability of endothelial cells to spontaneously form very small, branched and connected capillary networks directly interfacing parenchymal and stromal cells with intrinsic barrier function is so far unachieved by artificial fabrication technologies. However, their major shortcoming is the time consuming fabrication. Depending on the device size, four to ten days are required to accomplish complete vascular formation including anastomosis to the feeding channels. Additionally, only limited control over the cellular arrangement inside the bulk hydrogel is given, as was shown with the spontaneous spheroid formation of tumor cells[155].

Nevertheless, the power of this strategy lies in the versatility of fabrication approaches for the general device, where biomimetic and biosynthetic production technologies can be employed. Self-assembled microvascular networks advance these by adding another dimension of complexity and in vivo resemblance with round, branched vessels that form tight cellular junctions in the bulk material.

A detailed overview over the presented works based on self-assembled microvascular networks is given in Table 4 at the end of this review.

## 4. Summary and outlook

Organs-on-a-chip are an important tool for research on cell-cell interaction, matrix influence and of an organ's response to drug delivery. The inclusion of vasculature becomes especially critical for studies on drug reaction[40], tumor medication[29] and even virus uptake[160,161], since these mechanisms can only be realistically simulated with an endothelial lined vascular network.

In this review, a classification of vascularized OOC devices into biosynthetic, biomimetic and self-assembled vascular systems was presented. Biosynthetic devices spatially organize cells with synthetic materials in the area under investigation, while biomimetic OOCs try to mimic the native morphology with hydrogels. Devices that utilize the innate capability of endothelial cells to spontaneously form microvessel networks are describes as self-assembled microvascular systems.

This classification is not always clear-cut, as the transition is smooth, especially between self-assembled networks and biosynthetic fabrication approaches. In particular, the spatio-temporal region of interest for the planned cell biological and pharmacological investigation must be considered for the classification. As shown in this work, a biosynthetic or biomimetic chip design can

be vascularized by a self-assembled microvascular network after a couple of days[145,148]. If the interaction of the grown capillary network with the surrounding parenchyma is the focus of the planned study, such design would be considered as a self-assembled vascular OOC[48,155]. If the interface of the endothelial lined biosynthetic or biomimetic channel with adjacent cells marks the objective of the study, e.g. in tumor invasion studies[116] or endothelium-epithelium barrier studies[45,110], the OOC would be classified according to the definition of the originating channel type.

In general, biosynthetic approaches proved to be a good platform for studies of barrier functions, cell-cell interactions and cell behavior under flow conditions. The use of synthetic materials such as PDMS in the devices is critical, as synthetic materials show a strong small molecule absorbance, which possibly affects the outcome of quantitative biomolecule secretion studies[83]. Synthetic materials also possess mechanical properties different to native ECM, which influences cell proliferation and particularly stem cell differentiation[68]. Additional research is also required regarding the influence of the limited contact area of cells through the membrane pores or gaps in the channel walls. Although the application of synthetic material does not fully reflect the native tissue architecture, the biosynthetic OOCs presented proved to be a powerful and popular tool. Their primary strength originates from the fact that the properties of the synthetic barrier can be precisely controlled. Thus, cell-cell-signaling of different cell populations can be studied and modulated with high precision.

Biomimetic fabrication approaches aim to recreate the direct contact between vascular networks and parenchyma, and employ hydrogels with ECM-like mechanical and bioactive properties. In all presented works, the trade-off between minimum resolution and production speed in the fabrication of vasculature is apparent. The presented endothelial cell lined structures predominantly exhibited a diameter of more than 100 µm, demonstrating the limited spatial resolution of most bioprinting techniques[129]. In contrast, soft lithography and stereolithography printing offer feature sizes of only a few micrometers, but either require extensive manual work and expensive lithographic equipment to create micro-molds, or have a limited material selection with time-consuming ink-changing steps. Additionally, lithography is unable to create truly round shapes, either due to the rectangular mold or because of the minimum step size of SL printers[77]. This deviates from the natural vessel shape and affects flow dynamics. Whether this results in quantifiable and biofunctional restrictions should be subject of future research.

As of today, the presented biomimetic and biosynthetic fabrication approaches cannot produce both very fine and large vessels in a short time and in all three dimensions. Combining an engineered vessel network with self-assembled capillary networks is a solution to this size-problem. Branched, small and natively formed capillary networks can connect to the fabricated channel networks and provide direct cellular contact to parenchymal and stromal cells[159]. The presented studies demonstrated the great influence of the choice of endothelial and parenchymal cells on vessel morphology and gene expression[42,48].

This review showed that different technologies are available for vascularized OOC. This offers researchers a great variety of methods, but also demands careful consideration on which type of OOC design is best suited for the biological process under study. The interplay of materials, device layout, and cells is intricate and has proven to greatly influence cellular morphology, activity and proliferation. The question on the amount, the distribution and size of vascular channels required to gain robust results in quantitative studies also deserves attention for further research. Bodies-on-a-Chip add another level of complexity, since the interplay between various organs and possible toxicity of metabolic products on other parts of the human body is included. Vascularized Bodies-on-a-Chip have demonstrated that they yield pharmacokinetic parameters similar to those found in human patients and can play a valuable and meaningful role in pharmaceutical research[44,119].

These results highlight that research on complex vascular OOC devices has only just begun. There is still a long way ahead until the inclusion of vasculature into OOC devices will be a standard in research and development. Whether vascular OOC devices can one day successfully predict drug efficiency and therefore shorten expensive phase II clinical studies remains to be proven. If so, the much higher costs and time requirements compared to standardized, high-throughput screening assays could be compensated, and a gold-standard for future pharmaceutical research would be set.

## 5. Declaration of competing interest

The authors declare that they have no known competing financial interests or personal relationships that could have appeared to influence the work reported in this paper.

*Table 2: Overview over presented biosynthetic fabrication strategies.*

| Technology | Organ | Cells | Materials | Channel dimensions | Chamber / membrane dimensions | Authors |
|---|---|---|---|---|---|---|
| Membrane-based | Lung | A549 alveolar epithelial cells<br>primary murine alveolar epithelial cells | PDMS chip<br>PDMS membrane | 6 mm length<br>6 mm width | 100 µm membrane | [107] |
| | Kidney glomerulus | mice glomerular ECs<br>MPC-5 podocytes | PDMS chip<br>PC membrane<br>BME membrane coating | 100 µm height,<br>1000 µm width<br>10 mm length | 10 µm membrane<br>10 µm pores | [108] |
| | Kidney proximal tubule | primary proximal tubule epithelial cells | PDMS chip<br>polyester membrane<br>collagen IV membrane coating | 100 µm height<br>1000 µm width<br>1 cm length | 10 µm membrane<br>0.4 µm pores | [109] |
| | Lung | primary human airway epithelial cells<br>primary human lung microvascular ECs | PDMS chip<br>polyester membrane<br>collagen I membrane coating | 1000 µm width<br>200/1000 µm height<br>16.7 mm length | 10 µm membrane<br>0.4 µm pores | [110] |
| | Gut | intestinal epithelial cells Caco-2<br>lactobacillus rhamnosus | PDMS chip<br>PDMS membrane<br>collagen I + matrigel membrane coating | 150 µm height<br>1000 µm width | 30 µm membrane<br>10 µm pores | [112] |
| | Bone | primary bone marrow stromal cells<br>primary CD34+ hemapoetic stem cells | PDMS chip<br>PDMS membrane<br>fibrin + collagen membrane coating | 1 mm width<br>1 mm/200 µm height<br>16.7 mm length | 50 µm membrane<br>7 µm pores | [113] |
| | Gut/Liver/Kidney<br>Lung | HUVEC<br>primary liver sinusoidal microvascular ECs<br>A549 alveolar epithelial cells<br>pulmonary microvascular ECs<br>human primary hepatocytes<br>primary human renal proximal tubule epithelial cells<br>intestinal epithelial Caco-2 cells | PDMS chip<br>PDMS or PC membrane<br>fibrinogen, collagen I, matrigel coating | 400 µm width<br>100 µm length | 10 µm membrane<br>10 µm pores | [44,45,111] |
| Parallel channels | Breast cancer | osteodifferentiated human bone marrow-derived MSC<br>MDA-MB-231 human breast cancer cells<br>HUVEC | PDMS chip<br>poly-D-lysine channel coating<br>collagen I chamber filling | 150 µm width<br>120 µm height | 225 µm width | [115] |
| | Breast cancer | MDA-MB-231 human breast cancer<br>MCF-10A human mammary epithelial cells<br>human neonatal dermal fibroblasts<br>HUVEC | PDMS chip<br>collagen I | 120 µm height<br>300-440 µm width<br>3.2 mm length | 100 µm height<br>120 µm width | [116] |
| | Various cancer types | human fibrosarcoma HT1080<br>breast carcinoma MDA-MB-231<br>microvascular EC / HUVEC<br>murine macrophage cell line RAW264.7 | PDMS chip<br>collagen I | 500 µm width<br>1750 µm length<br>240 µm height | 750 µm width | [117] |
| | Blood-brain-barrier | human primary cerebral microvascular ECs<br>primary rat astocytes + neurons | PDMS chip<br>collagen I<br>poly-D-lysine channel coating | 920 µm width<br>190 µm height<br>4.36 mm length | 580 µm width | [104] |
| Polymer sheet stamping | Liver<br>Myocardium | HUVEC<br>hMSC<br>hESC derived hepatocytes<br>primary rat hepatocytes<br>neonatal rat cardiomyocytes | POMaC<br>PDMS and PC chip<br>gelatin coating of channels<br>matrigel chamber | 100 µm height<br>100 µm width | 5 x 3.2 $mm^2$<br>700 µm height<br>20 - 100 µm pores<br>25 µm membrane | [118] |
| | Liver<br>Myocardium<br>Breast cancer | HUVEC<br>HepG2<br>hiPSC derived cardiomyocytes<br>breast cancer cell line MDA-MB-231 | POMaBC<br>PDMS and PC chip<br>gelatin coating of channels<br>fibrin gel chamber | 100 µm width<br>100 µm height | 4 x 3 x 2 $mm^3$<br>15 µm pores<br>50 µm membrane | [119] |

*Table 3: Overview over presented biomimetic fabrication strategies.*

| Production method | Organ | Cells | Materials | Minimum vessel size | Device size | Authors |
|---|---|---|---|---|---|---|
| Soft lithography | Liver | AML-12 hepatocytes | agarose | 50 x 70 µm | 1.25 mm x 1.25 mm x 3 cm | [120] |
| | Skin | human dermal microvascular ECs<br>human dermal fibroblasts | sacrificial gelatin<br>casted collagen I/fibrin/matrigel | 6 - 50 µm | 10 $mm^2$, 1 mm deep | [43] |
| | Blood vessel | HUVEC<br>human brain perivascular cells<br>human umbilical arterial SMC | sacrificial gelatin<br>casted collagen I | 100 x 100 µm | 20 x 20 x 1.2 $mm^3$ | [122] |
| | Liver | HepG2<br>HUVEC | agarose<br>collagen I coating | 30 x 150 µm | leaf size ($cm^2$ area) | [121] |
| | Liver | HepG2 | PDMS device<br>casted collagen I | < 30 µm diameter | 500 µm culture chamber diameter<br>leaf size ($cm^2$ area) | [123] |
| | Liver<br>Bone<br>Cancer | HepG2<br>hMSC<br>HUVEC<br>PANC-1 cancer cells | PDMS device<br>casted fibrin | < 30 µm diameter | 2 mm culture chamber diameter<br>leaf size ($cm^2$ area) | [124] |
| Needle casting | Blood vessel | HUVEC<br>rat aortic SMCs<br>3T3 fibroblasts | GelMA | 120 µm inner diameter<br>500 µm layer thickness<br>1.2 mm outer diameter | 15 mm length | [126] |
| | Blood vessel | HUVEC<br>human dermal microvascular ECs<br>human perivascular cells | collagen I | 75 - 150 µm | 1 mm x 1 mm x 1 cm | [125] |
| 3D printed fiber pulling | Bone | MC3T3 mouse pre-osteoblasts<br>HUVEC | agarose<br>casted GelMA, PEG-DA, PEGDMA, SPELA | 150 - 500 µm | approx. 10 x 10 x 3 $mm^3$ | [127] |
| | Liver | HepG2 | agarose<br>casted GelMA | 100 µm | 1 x 2 x 0.5 $cm^3$ | [128] |
| Coaxial nozzle printing | Blood vessel | HUVEC<br>hMSC | alginate-GelMA-PEG-TA | 400 µm inner<br>500 µm outer | 8 x 9 x 7 $mm^3$ | [52] |
| | Blood vessel<br>Urethelium | HUVEC<br>hMSC<br>urothelial cells + urethelial SMC | GelMA<br>alginate<br>PEG acrylate | 600 µm inner<br>1000 µm outer | centimeter length | [62] |
| Sacrificial extrusion printing | Liver | HUVEC<br>HepG2 | sacrificial gelatin<br>collagen I<br>PCL-printed chip | 200 µm | 1.5 x 1.5 x 15 $mm^3$ | [91] |
| | Blood vessel | HUVEC<br>10T1/2 mouse fibroblast<br>Human neonatal dermal fibroblasts | sacrificial Pluronic F-127<br>GelMA | 150 µm | 15 x 15 x 1 $mm^3$ | [133] |
| | Blood vessel<br>Bone | HUVEC<br>hMSC - differentiated into osteoblasts<br>Human neonatal dermal fibroblasts | sacrificial Pluronic F-127<br>gelatin-fibrin | 600 µm | 10 $cm^3$ | [132] |
| | Kidney | RPTEC/TERT1 proximal tubule epithelial cells<br>Human neonatal dermal fibroblasts<br>glomerular microvascular ECs | sacrificial Pluronic F-127<br>gelatin-fibrin-transglutamase | 400 µm | centimeter length | [134,135] |
| | Liver | HUVEC<br>primary rat hepatocytes | sacrificial carbohydrate-dextran glass<br>agarose, PEG, alginate, fibrin | 100 µm | 10 x 20 x 2.4 $mm^3$ | [136] |

| | | | | | | |
|---|---|---|---|---|---|---|
| Microvalve drop printing | Blood vessel | HUVEC<br>human umbilical artery SMCs<br>human dermal normal fibroblasts | sacrificial gelatin<br>fibrin-collagen coating<br>casted collagen | 600 µm | 16 x 1.5 x 1 $mm^3$ | [27] |
| Microvalve drop printing<br>Extrusion printing | Brain<br>Cancer | murine neural progenitor cells<br>hiPSC derived cortical neural progenitor cells<br>HUVEC<br>breast cancer epithelial spheroids (CF10AT) | sacrificial gelatin<br>RGD-modified elastin-like protein | 2 mm | 8 mm height<br>5 mm diameter | [131] |
| Stereolithography printing | Liver | HUVEC<br>C3H/10T1/2 mouse fibroblasts<br>HepG2 | GelMA<br>GelMA + hyaluronic acid | 5 - 250 µm | 4 mm x 5 mm x 600 µm | [137] |
| | Lung<br>Bone<br>Live | human normal lung fibroblasts<br>human lung epithelial cells<br>hMSC<br>HUVEC<br>human neonatal dermal fibroblasts<br>primary rat hepatocytes | PEG-DA + Gel-MA | 250 µm | 16 x 10 x 4 $mm^3$ | [138] |

*Table 4: Overview over presented self-assembled microvascular networks.*

| Technology | Production method | Organ | Cells | Materials | Channel dimensions | Chamber dimensions | Author |
|---|---|---|---|---|---|---|---|
| Parallel channels | PDMS soft lithography | Blood-brain-barrier | HUVEC<br>human normal lung fibroblasts<br>rat cortical neurons | PDMS chip<br>casted fibrin | 100 µm gaps | 750 µm width | [143] |
| | | Blood-brain-barrier | hiPSC derived ECs<br>brain pericytes<br>astrocytes | fibrin coated PDMS channels<br>fibrin casted gel | 1000 µm width<br>150 µm height<br>200 µm gaps | 1300 µm width<br>150 µm height | [48] |
| | | Cancer | human normal lung fibroblasts<br>endothelial colony-forming cell-derived EC<br>colorectal / melanoma / breast cancer cells | fibrin casted gel<br>laminin coated PDMS channels | 100 x 100 µm$^2$<br>50 µm gaps | 1 x 2 mm$^2$ diamond<br>100 µm height | [155,156] |
| | Injection molding | Blood vessel<br>Brain cancer | HUVEC<br>human normal lung fibroblasts<br>brain glioblastoma U87MG | PS chip<br>PS well plate<br>casted fibrin | 100 µm height<br>2 mm width | 1.5 mm height<br>800 µm width<br>7 mm length | [103,158] |
| | | Brain | human brain microvascular ECs<br>human normal lung fibroblasts<br>human astrocytes<br>rat primary neurons + schwann cells | PS chip<br>PS well plate<br>casted fibrin | 100 µm height<br>1 mm width<br>100 µm gaps | 1 mm width<br>100 µm height<br>7 mm length | [159] |
| | 3D extrusion printing | Blood vessel | HUVEC<br>human normal lung / dermal fibroblast | sacrificial gelatin<br>collagen / fibrin | 400 µm x 110 µm | 3 mm x 12 mm | [139,144,145] |
| Parallel channels + membrane-based | PDMS soft lithography | fat<br>retina<br>cancer | human normal lung fibroblasts<br>HUVEC<br>human adipose microvascular ECs<br>retinal ECs + ocular choroid fibroblasts<br>iPSC retinal pigment epithelial cells<br>A549 human lung adenocarcinoma spheroid | PDMS chip<br>casted fibrin / fibrin-collagen I | 400 µm diameter | 1600 µm length<br>400 µm height<br>400 µm width<br>1 x 3 mm connection top | [42] |
| | 3D extrusion printing | alveoli | human dermal microvascular ECs<br>human normal lung fibroblasts<br>primary human tracheal epithelial cells | PCL printed chambers<br>printed decellularized ECM<br>collagen I | 300 µm height<br>2 mm width | 36 mm length<br>5 mm width<br>300 µm height | [162] |

# 6. Literature


1 Bugrim A, Nikolskaya T, Nikolsky Y. Early prediction of drug metabolism and toxicity : systems biology approach and modeling and suggest directions for their integration . *Drug Discov Today* 2004; **9**: 127–135.

2 Esch MB, Prot JM, Wang YI, Miller P, Llamas-Vidales JR, Naughton BA *et al.* Multi-cellular 3D human primary liver cell culture elevates metabolic activity under fluidic flow. *Lab Chip* 2015; **15**: 2269–2277.

3 Fetah K, Tebon P, Goudie MJ, Eichenbaum J, Ren L, Barros N *et al.* The emergence of 3D bioprinting in organ-on-chip systems. *Prog Biomed Eng* 2019; **1**: 012001.

4 Ewart L, Dehne E-M, Fabre K, Gibbs S, Hickman J, Hornberg E *et al.* Application of Microphysiological Systems to Enhance Safety Assessment in Drug Discovery. *Annu Rev Pharmacol Toxicol* 2018; **58**: 65–82.

5 Paul SM, Mytelka DS, Dunwiddie CT, Persinger CC, Munos BH, Lindborg SR *et al.* How to improve RD productivity: The pharmaceutical industry's grand challenge. *Nat Rev Drug Discov* 2010; **9**: 203–214.

6 Breslin S, O'Driscoll L. Three-dimensional cell culture: The missing link in drug discovery. *Drug Discov Today* 2013; **18**: 240–249.

7 Baudoin R, Griscom L, Prot JM, Legallais C, Leclerc E. Behavior of HepG2/C3A cell cultures in a microfluidic bioreactor. *Biochem Eng J* 2011; **53**: 172–181.

8 Albanese A, Lam AK, Sykes EA, Rocheleau J V., Chan WCW. Tumour-on-a-chip provides an optical window into nanoparticle tissue transport. *Nat Commun* 2013; **4**: 1–8.

9 Tostões RM, Leite SB, Serra M, Jensen J, Björquist P, Carrondo MJT *et al.* Human liver cell spheroids in extended perfusion bioreactor culture for repeated-dose drug testing. *Hepatology* 2012; **55**: 1227–1236.

10 Wu LY, Di Carlo D, Lee LP. Microfluidic self-assembly of tumor spheroids for anticancer drug discovery. *Biomed Microdevices* 2008; **10**: 197–202.

11 Lee SA, No DY, Kang E, Ju J, Kim DS, Lee SH. Spheroid-based three-dimensional liver-on-a-chip to investigate hepatocyte-hepatic stellate cell interactions and flow effects. *Lab Chip* 2013; **13**: 3529–3537.

12 Norotte C, Marga FS, Niklason LE, Forgacs G. Scaffold-free vascular tissue engineering using bioprinting. *Biomaterials* 2009; **30**: 5910–5917.

13 Kizawa H, Nagao E, Shimamura M, Zhang G, Torii H. Scaffold-free 3D bio-printed human liver tissue stably maintains metabolic functions useful for drug discovery. *Biochem Biophys Reports* 2017; **10**: 186–191.

14 Kim J, Koo BK, Knoblich JA. Human organoids: model systems for human biology and medicine. *Nat Rev Mol Cell Biol* 2020; **21**. doi:10.1038/s41580-020-0259-3.

15 Xinaris C, Brizi V, Remuzzi G. Organoid Models and Applications in Biomedical Research. *Nephron* 2015; **130**: 191–199.

16 Wörsdörfer P, Dalda N, Kern A, Krüger S, Wagner N, Kwok CK *et al.* Generation of complex human organoid models including vascular networks by incorporation of mesodermal progenitor cells. *Sci Rep* 2019; **9**: 1–13.

17 Homan KA, Gupta N, Kroll KT, Kolesky DB, Skylar-Scott M, Miyoshi T *et al.* Flow-enhanced

vascularization and maturation of kidney organoids in vitro. *Nat Methods* 2019; **16**: 255–262.

18 Huh D, Hamilton GA, Ingber DE. From 3D cell culture to organs-on-chips. *Trends Cell Biol* 2011; **21**: 745–754.

19 Bhatia SN, Ingber DE. Microfluidic organs-on-chips. *Nat Biotechnol* 2014; **32**: 760–772.

20 Van Midwoud PM, Verpoorte E, Groothuis GMM. Microfluidic devices for in vitro studies on liver drug metabolism and toxicity. *Integr Biol* 2011; **3**: 509–521.

21 Ghaemmaghami AM, Hancock MJ, Harrington H, Kaji H, Khademhosseini A. Biomimetic tissues on a chip for drug discovery. *Drug Discov Today* 2012; **17**: 173–181.

22 Ashammakhi N, Ahadian S, Xu C, Montazerian H, Ko H, Nasiri R *et al.* Bioinks and bioprinting technologies to make heterogeneous and biomimetic tissue constructs. *Mater Today Bio* 2019; **1**: 100008.

23 Unagolla JM, Jayasuriya AC. Hydrogel-based 3D bioprinting: A comprehensive review on cell-laden hydrogels, bioink formulations, and future perspectives. *Appl Mater Today* 2019; : 100479.

24 Bhise NS, Ribas J, Manoharan V, Zhang YS, Polini A, Massa S *et al.* Organ-on-a-chip platforms for studying drug delivery systems. *J Control Release* 2014; **190**: 82–93.

25 Jain RK, Au P, Tam J, Duda DG, Fukumura D. Engineering vascularized tissue. *Nat Biotechnol* 2005; **23**: 821–823.

26 Bogorad MI, DeStefano J, Karlsson J, Wong AD, Gerecht S, Searson PC. Review: In vitro microvessel models. *Lab Chip* 2015; **15**: 4242–4255.

27 Schöneberg J, De Lorenzi F, Theek B, Blaeser A, Rommel D, Kuehne AJC *et al.* Engineering biofunctional in vitro vessel models using a multilayer bioprinting technique. *Sci Rep* 2018; **8**: 1–13.

28 Poisson J, Lemoinne S, Boulanger C, Durand F, Moreau R, Valla D *et al.* Liver sinusoidal endothelial cells: Physiology and role in liver diseases. *J Hepatol* 2017; **66**: 212–227.

29 Caballero D, Blackburn SM, De Pablo M, Samitier J, Albertazzi L. Tumour-vessel-on-a-chip models for drug delivery. *Lab Chip* 2017; **17**: 3760–3771.

30 Stroock AD, Fischbach C. Microfluidic culture models of tumor angiogenesis. *Tissue Eng - Part A* 2010; **16**: 2143–2146.

31 Majno G. Ultrastructure of the vascular membrane. In: Hamilton EF, Dow D (eds). *Handbook of Physiology*. American Physiological Society: Washington, D.C., 1965, pp 2293–2375.

32 Paulsen SJ, Miller JS. Tissue vascularization through 3D printing: Will technology bring us flow? *Dev Dyn* 2015; **244**: 629–640.

33 Bassenge E. Endothelial function in different organs. *Prog Cardiovasc Dis* 1996; **39**: 209–228.

34 Embry AE, Mohammadi H, Niu X, Liu L, Moe B, Miller-Little WA *et al.* Biochemical and cellular determinants of renal glomerular elasticity. *PLoS One* 2016; **11**: 1–25.

35 Lin DSY, Guo F, Zhang B. Modeling organ-specific vasculature with organ-on-a-chip devices. *Nanotechnology* 2019; **30**. doi:10.1088/1361-6528/aae7de.

36 Aird WC. Phenotypic heterogeneity of the endothelium: I. Structure, function, and mechanisms. *Circ Res* 2007; **100**: 158–173.

37 Wong AD, Ye M, Levy AF, Rothstein JD, Bergles DE, Searson PC. The blood-brain barrier: An

engineering perspective. *Front Neuroeng* 2013; **6**: 1–22.

38 Braverman IM. The cutaneous microcirculation. *J Investig Dermatology Symp Proc* 2000; **5**: 3–9.

39 Yamanaka S. Induced pluripotent stem cells: Past, present, and future. *Cell Stem Cell* 2012; **10**: 678–684.

40 Ronaldson-Bouchard K, Vunjak-Novakovic G. Organs-on-a-Chip: A Fast Track for Engineered Human Tissues in Drug Development. *Cell Stem Cell* 2018; **22**: 310–324.

41 Ahadian S, Civitarese R, Bannerman D, Mohammadi MH, Lu R, Wang E *et al.* Organ-On-A-Chip Platforms: A Convergence of Advanced Materials, Cells, and Microscale Technologies. *Adv Healthc Mater* 2018; **7**: 1–53.

42 Paek J, Park SE, Lu Q, Park KT, Cho M, Oh JM *et al.* Microphysiological Engineering of Self-Assembled and Perfusable Microvascular Beds for the Production of Vascularized Three-Dimensional Human Microtissues. *ACS Nano* 2019; **13**: 7627–7643.

43 Golden AP, Tien J. Fabrication of microfluidic hydrogels using molded gelatin as a sacrificial element. *Lab Chip* 2007; **7**: 720–725.

44 Herland A, Maoz BM, Das D, Somayaji MR, Prantil-Baun R, Novak R *et al.* Quantitative prediction of human pharmacokinetic responses to drugs via fluidically coupled vascularized organ chips. *Nat Biomed Eng* 2020; : 1–16.

45 Huh D, Matthews BD, Mammoto A, Montoya-Zavala M, Hsin HY, Ingber DE. Reconstituting Organ-Level Lung Functions on a Chip. *Science (80- )* 2010; : 1662–1668.

46 Novak R, Ingram M, Marquez S, Das D, Delahanty A, Herland A *et al.* Robotic fluidic coupling and interrogation of multiple vascularized organ chips. *Nat Biomed Eng* 2020; : 1–14.

47 Aird WC. Endothelial Cell Heterogeneity. *Cold Spring Harb Perspect Med* 2012; **2**. doi:10.1101/cshperspect.a006429.

48 Campisi M, Shin Y, Osaki T, Hajal C, Chiono V, Kamm RD. 3D self-organized microvascular model of the human blood-brain barrier with endothelial cells, pericytes and astrocytes. *Biomaterials* 2018; **180**: 117–129.

49 Kosyakova N, Kao DD, Figetakis M, López-Giráldez F, Spindler S, Graham M *et al.* Differential functional roles of fibroblasts and pericytes in the formation of tissue-engineered microvascular networks in vitro. *npj Regen Med* 2020; **5**. doi:10.1038/s41536-019-0086-3.

50 Mayer H, Bertram H, Lindenmaier W, Korff T, Weber H, Weich H. Vascular endothelial growth factor (VEGF-A) expression in human mesenchymal stem cells: Autocrine and paracrine role on osteoblastic and endothelial differentiation. *J Cell Biochem* 2005; **95**: 827–839.

51 Caplan AI. Mesenchymal stem cells: Time to change the name! *Stem Cells Transl Med* 2017; **6**: 1445–1451.

52 Jia W, Gungor-Ozkerim PS, Zhang YS, Yue K, Zhu K, Liu W *et al.* Direct 3D bioprinting of perfusable vascular constructs using a blend bioink. *Biomaterials* 2016; **106**: 58–68.

53 Liu H, Wang Y, Cui K, Guo Y, Zhang X, Qin J. Advances in Hydrogels in Organoids and Organs-on-a-Chip. *Adv Mater* 2019; **31**: 1–28.

54 Carlini AS, Adamiak L, Gianneschi NC. Biosynthetic polymers as functional materials. *Macromolecules* 2016; **49**: 4379–4394.

55 Patterson J, Martino MM, Hubbell JA. Biomimetic materials in tissue engineering. *Mater*

*Today* 2010; **13**: 14–22.

56 Skardal A. Bioprinting Essentials of cell and protein viability. In: *Essentials of 3D Biofabrication and Translation*. Elsevier, 2015, pp 1–17.

57 Moon JJ, Saik JE, Poché RA, Leslie-Barbick JE, Lee SH, Smith AA *et al.* Biomimetic hydrogels with pro-angiogenic properties. *Biomaterials* 2010; **31**: 3840–3847.

58 Leslie-Barbick JE, Saik JE, Gould DJ, Dickinson ME, West JL. The promotion of microvasculature formation in poly(ethylene glycol) diacrylate hydrogels by an immobilized VEGF-mimetic peptide. *Biomaterials* 2011; **32**: 5782–5789.

59 Blaeser A, Million N, Campos DFD, Gamrad L, Köpf M, Rehbock C *et al.* Laser-based in situ embedding of metal nanoparticles into bioextruded alginate hydrogel tubes enhances human endothelial cell adhesion. *Nano Res* 2016; **9**: 3407–3427.

60 Li Y, Rehbock C, Nachev M, Stamm J, Sures B, Blaeser A *et al.* Matrix-specific mechanism of Fe ion release from laser-generated 3D-printable nanoparticle-polymer composites and their protein adsorptionproperties. *Nanotechnology* 2020. doi:https://doi.org/10.1088/1361-6528/ab94da.

61 Tsang VL, Chen AA, Cho LM, Jadin KD, Sah RL, DeLong S *et al.* Fabrication of 3D hepatic tissues by additive photopatterning of cellular hydrogels. *FASEB J* 2007; **21**: 790–801.

62 Pi Q, Maharjan S, Yan X, Liu X, Singh B, van Genderen AM *et al.* Digitally Tunable Microfluidic Bioprinting of Multilayered Cannular Tissues. *Adv Mater* 2018; **30**: 1–10.

63 Noor N, Shapira A, Edri R, Gal I, Wertheim L, Dvir T. 3D Printing of Personalized Thick and Perfusable Cardiac Patches and Hearts. *Adv Sci* 2019; **6**. doi:10.1002/advs.201900344.

64 Kim J, Shim IK, Hwang DG, Lee YN, Kim M, Kim H *et al.* 3D cell printing of islet-laden pancreatic tissue-derived extracellular matrix bioink constructs for enhancing pancreatic functions. *J Mater Chem B* 2019; **7**: 1773–1781.

65 Wolchok JC, Tresco PA. The isolation of cell derived extracellular matrix constructs using sacrificial open-cell foams. *Biomaterials* 2010; **31**: 9595–9603.

66 Hielscher AC, Qiu C, Gerecht S. Breast cancer cell-derived matrix supports vascular morphogenesis. *Am J Physiol - Cell Physiol* 2012; **302**. doi:10.1152/ajpcell.00011.2012.

67 Lu H, Hoshiba T, Kawazoe N, Koda I, Song M, Chen G. Cultured cell-derived extracellular matrix scaffolds for tissue engineering. *Biomaterials* 2011; **32**: 9658–9666.

68 Skardal A, Mack D, Atala A, Sokern S. Substrate elasticity controls cell proliferation, surface marker expression and motile phenotype in amniotic fluid-derived stem cells. *J Mech Behav Biomed Mater* 2013; **17**: 307–316.

69 Engler AJ, Sen S, Sweeney HL, Discher DE. Matrix Elasticity Directs Stem Cell Lineage Specification. *Cell* 2006; **126**: 677–689.

70 Lai-Fook SJ, Hyatt RE. Effects of age on elastic moduli of human lungs. *J Appl Physiol* 2000; **89**: 163–168.

71 Murphy MC. Decreased brain stiffness in Alzheimer's Disease determined by MRE. 2012; **34**: 494–498.

72 Yeh WC, Li PC, Jeng YM, Hsu HC, Kuo PL, Li ML *et al.* Elastic modulus measurements of human liver and correlation with pathology. *Ultrasound Med Biol* 2002; **28**: 467–474.

73 Shen J, Xie Y, Liu Z, Zhang S, Wang Y, Jia L *et al.* Increased myocardial stiffness activates

cardiac microvascular endothelial cell via VEGF paracrine signaling in cardiac hypertrophy. *J Mol Cell Cardiol* 2018; **122**: 140–151.

74 Wells R. Tissue Mechanics and Fibrosis. *Wells, Rebecca G 'Tissue Mech fibrosis' Biochim Biophys Acta* 2013; **1832**: 884–890.

75 Miri AK, Khalilopour A, Cecen B, Maharjan S, Shin SR, Khademhosseini A. Multiscale bioprinting of vascularized models. *Biomaterials* 2019; **198**: 204–219.

76 Parak A, Pradeep P, du Toit LC, Kumar P, Choonara YE, Pillay V. Functionalizing bioinks for 3D bioprinting applications. *Drug Discov Today* 2019; **24**: 198–205.

77 Miri AK, Mostafavi E, Khorsandi D, Hu SK, Malpica M, Khademhosseini A. Bioprinters for organs-on-chips. *Biofabrication* 2019; **11**. doi:10.1088/1758-5090/ab2798.

78 Kreimendahl F, Köpf M, Thiebes AL, Duarte Campos DF, Blaeser A, Schmitz-Rode T *et al.* Three-Dimensional Printing and Angiogenesis: Tailored Agarose-Type i Collagen Blends Comprise Three-Dimensional Printability and Angiogenesis Potential for Tissue-Engineered Substitutes. *Tissue Eng - Part C Methods* 2017; **23**: 604–615.

79 Köpf M, Campos DFD, Blaeser A, Sen KS, Fischer H. A tailored three-dimensionally printable agarose-collagen blend allows encapsulation, spreading, and attachment of human umbilical artery smooth muscle cells. *Biofabrication* 2016; **8**: 1–15.

80 Goetzke R, Franzen J, Ostrowska A, Vogt M, Blaeser A, Klein G *et al.* Does soft really matter? Differentiation of induced pluripotent stem cells into mesenchymal stromal cells is not influenced by soft hydrogels. *Biomaterials* 2018; **156**: 147–158.

81 Borenstein JT, Terai H, King KR, Weinberg EJ, Kaazempur-Mofrad MR, Vacanti JP. Microfabrication technology for vascularized tissue engineering. *Biomed Microdevices* 2002; **4**: 167–175.

82 Annabi N, Selimović Š, Acevedo Cox JP, Ribas J, Afshar Bakooshli M, Heintze D *et al.* Hydrogel-coated microfluidic channels for cardiomyocyte culture. *Lab Chip* 2013; **13**: 3569–3577.

83 Wang JD, Douville NJ, Takayama S, Elsayed M. Quantitative analysis of molecular absorption into PDMS microfluidic channels. *Ann Biomed Eng* 2012; **40**: 1862–1873.

84 Toepke MW, Beebe DJ. PDMS absorption of small molecules and consequences in microfluidic applications. *Lab Chip* 2006; **6**: 1484–1486.

85 van Meer BJ, de Vries H, Firth KSA, van Weerd J, Tertoolen LGJ, Karperien HBJ *et al.* Small molecule absorption by PDMS in the context of drug response bioassays. *Biochem Biophys Res Commun* 2017; **482**: 323–328.

86 Zhou J, Ellis AV, Voelcker NH. Recent developments in PDMS surface modification for microfluidic devices. *Electrophoresis* 2010; **31**: 2–16.

87 Sibarani J, Takai M, Ishihara K. Surface modification on microfluidic devices with 2-methacryloyloxyethyl phosphorylcholine polymers for reducing unfavorable protein adsorption. *Colloids Surfaces B Biointerfaces* 2007; **54**: 88–93.

88 Li L, Hitchcock AP, Robar N, Cornelius R, Brash JL, Scholl A *et al.* X-ray microscopy studies of protein adsorption on a phase-segregated polystyrene/polymethyl methacrylate surface. 1. Concentration and exposure-time dependence for albumin adsorption. *J Phys Chem B* 2006; **110**: 16763–16773.

89 Li N, Schwartz M, Ionescu-Zanetti C. PDMS compound adsorption in context. *J Biomol Screen* 2009; **14**: 194–202.

90 Hirama H, Satoh T, Sugiura S, Shin K, Onuki-Nagasaki R, Kanamori T *et al.* Glass-based organ-on-a-chip device for restricting small molecular absorption. *J Biosci Bioeng* 2019; **127**: 641–646.

91 Lee H, Cho DW. One-step fabrication of an organ-on-a-chip with spatial heterogeneity using a 3D bioprinting technology. *Lab Chip* 2016; **16**: 2618–2625.

92 Ausoni S, Sartore S. The cardiovascular unit as a dynamic player in disease and regeneration. *Trends Mol Med* 2009; **15**: 543–552.

93 Knudsen L, Ochs M. The micromechanics of lung alveoli: structure and function of surfactant and tissue components. *Histochem Cell Biol* 2018; **150**: 661–676.

94 Scott RP, Quaggin SE. The cell biology of renal filtration. *J Cell Biol* 2015; **209**: 199–210.

95 Haschek W, Rousseaux C, Wallig M. Chapter 9 - The Liver. In: *Fundamentals of Toxicologic Pathology (Second edition)*. Academic Press, 2017, pp 197–235.

96 Maina JN, West JB. Thin and strong! The bioengineering dilemma in the structural and functional design of the blood-gas barrier. *Physiol Rev* 2005; **85**: 811–844.

97 Xu L, Nirwane A, Yao Y. Basement membrane and blood-brain barrier. *Stroke Vasc Neurol* 2019; **4**: 78–82.

98 Villemain O, Correia M, Mousseaux E, Baranger J, Zarka S, Podetti I *et al.* Myocardial Stiffness Evaluation Using Noninvasive Shear Wave Imaging in Healthy and Hypertrophic Cardiomyopathic Adults. *JACC Cardiovasc Imaging* 2019; **12**: 1135–1145.

99 Pollak MR, Quaggin SE, Hoenig MP, Dworkin LD. The glomerulus: The sphere of influence. *Clin J Am Soc Nephrol* 2014; **9**: 1461–1469.

100 Low L, Mummery C, Berridge BR, Austin CP, Tagle DA. Organs-on-chips: into the next decade. *Nat Rev Drug Discov* 2020; : 1–17.

101 Caballero D, Kaushik S, Correlo VM, Oliveira JM, Reis RL, Kundu SC. Organ-on-chip models of cancer metastasis for future personalized medicine: From chip to the patient. *Biomaterials* 2017; **149**: 98–115.

102 Wang G, McCain ML, Yang L, He A, Pasqualini FS, Agarwal A *et al.* Modeling the mitochondrial cardiomyopathy of Barth syndrome with induced pluripotent stem cell and heart-on-chip technologies. *Nat Med* 2014; **20**: 616–623.

103 Ko J, Ahn J, Kim S, Lee Y, Lee J, Park D *et al.* Tumor spheroid-on-a-chip: A standardized microfluidic culture platform for investigating tumor angiogenesis. *Lab Chip* 2019; **19**: 2822–2833.

104 Adriani G, Ma D, Pavesi A, Kamm RD, Goh ELK. A 3D neurovascular microfluidic model consisting of neurons, astrocytes and cerebral endothelial cells as a blood–brain barrier. *Lab Chip* 2017; : 448–459.

105 Nam K, Smith AST, Lone S, Kwon S. Biomimetic three-dimensional tissue models for advanced high-throughput drug screening. *J Lab Autom* 2015; **20**: 201–215.

106 Cuchiara MP, Gould DJ, McHale MK, Dickinson ME, West JL. Integration of self-assembled microvascular networks with microfabricated PEG-based hydrogels. *Adv Funct Mater* 2012; **22**: 4511–4518.

107 Douville NJ, Zamankhan P, Tung YC, Li R, Vaughan BL, Tai CF *et al.* Combination of fluid and solid mechanical stresses contribute to cell death and detachment in a microfluidic alveolar model. *Lab Chip* 2011; **11**: 609–619.

108 Zhou M, Zhang X, Wen X, Wu T, Wang W, Yang M *et al.* Development of a Functional Glomerulus at the Organ Level on a Chip to Mimic Hypertensive Nephropathy. *Sci Rep* 2016; **6**: 1–13.

109 Jang KJ, Mehr AP, Hamilton GA, McPartlin LA, Chung S, Suh KY *et al.* Human kidney proximal tubule-on-a-chip for drug transport and nephrotoxicity assessment. *Integr Biol (United Kingdom)* 2013; **5**: 1119–1129.

110 Benam KH, Villenave R, Lucchesi C, Varone A, Hubeau C, Lee HH *et al.* Small airway-on-a-chip enables analysis of human lung inflammation and drug responses in vitro. *Nat Methods* 2016; **13**: 151–157.

111 Huh D, Kim HJ, Fraser JP, Shea DE, Khan M, Bahinski A *et al.* Microfabrication of human organs-on-chips. *Nat Protoc* 2013; **8**: 2135–2157.

112 Kim HJ, Huh D, Hamilton G, Ingber DE. Human gut-on-a-chip inhabited by microbial flora that experiences intestinal peristalsis-like motions and flow. *Lab Chip* 2012; **12**: 2165–2174.

113 Chou DB, Frismantas V, Milton Y, David R, Pop-Damkov P, Ferguson D *et al.* On-chip recapitulation of clinical bone marrow toxicities and patient-specific pathophysiology. *Nat Biomed Eng* 2020; : 394–406.

114 Novak R, Ingram M, Marquez S, Das D, Delahanty A, Herland A *et al.* Robotic fluidic coupling and interrogation of multiple vascularized organ chips. *Nat Biomed Eng* 2020; : 1–14.

115 Bersini S, Jeon JS, Dubini G, Arrigoni C, Chung S, Charest JL *et al.* A microfluidic 3D in vitro model for specificity of breast cancer metastasis to bone. *Biomaterials* 2014; **35**: 2454–2461.

116 Du Z, Mi S, Yi X, Xu Y, Sun W. Microfluidic system for modelling 3D tumour invasion into surrounding stroma and drug screening. *Biofabrication* 2018; **10**. doi:https://doi.org/10.1088/1758-5090/aac70c.

117 Zervantonakis IK, Hughes-alford SK, Charest JL, Condeelis JS. Three-dimensional microfluidic model for tumor cell intravasation and endothelial barrier function. *Proc Natl Acad Sci U S A* 2012. doi:10.1073/pnas.1210182109.

118 Zhang B, Montgomery M, Chamberlain MD, Ogawa S, Korolj A, Pahnke A *et al.* Biodegradable scaffold with built-in vasculature for organ-on-a-chip engineering and direct surgical anastomosis. *Nat Mater* 2016; **15**: 669–678.

119 Lai BFL, Huyer LD, Lu RXZ, Drecun S, Radisic M, Zhang B. InVADE: Integrated Vasculature for Assessing Dynamic Events. *Adv Funct Mater* 2017; **27**: 1–11.

120 Ling Y, Rubin J, Deng Y, Huang C, Demirci U, Karp JM *et al.* A cell-laden microfluidic hydrogel. *Lab Chip* 2007; **7**: 756–762.

121 He J, Mao M, Liu Y, Shao J, Jin Z, Li D. Fabrication of nature-inspired microfluidic network for perfusable tissue constructs. *Adv Healthc Mater* 2013; **2**: 1108–1113.

122 Zheng Y, Chen J, Craven M, Choi NW, Totorica S, Diaz-Santana A *et al.* In vitro microvessels for the study of angiogenesis and thrombosis. *Proc Natl Acad Sci U S A* 2012; **109**: 9342–9347.

123 Mao M, He J, Lu Y, Li X, Li T, Zhou W *et al.* Leaf-templated, microwell-integrated microfluidic chips for high-throughput cell experiments. *Biofabrication* 2018; **10**: 25008.

124 Mao M, Bei HP, Lam CH, Chen P, Wang S, Chen Y *et al.* Human-on-Leaf-Chip: A Biomimetic Vascular System Integrated with Chamber-Specific Organs. *Small* 2020; **16**: 1–11.

125 Chrobak KM, Potter DR, Tien J. Formation of perfused, functional microvascular tubes in vitro. *Microvasc Res* 2006; **71**: 185–196.

126 Hasan A, Paul A, Memic A, Khademhosseini A. A multilayered microfluidic blood vessel-like structure. *Biomed Microdevices* 2015; **17**: 1–13.

127 Bertassoni L, Cecconi M, Manoharan V, Nikkhah M, Yang Y, Khademhosseini A. Hydrogel bioprinted microchannel networks for vascularization of tissue engineering constructs. *Lab Chip* 2014; **14**: 2202–2211.

128 Massa S, Sakr MA, Seo J, Bandaru P, Arneri A, Bersini S *et al.* Bioprinted 3D vascularized tissue model for drug toxicity analysis. *Biomicrofluidics* 2017; **11**. doi:10.1063/1.4994708.

129 Matai I, Kaur G, Seyedsalehi A, McClinton A, Laurencin CT. Progress in 3D bioprinting technology for tissue/organ regenerative engineering. *Biomaterials* 2020; **226**: 119536.

130 Ma X, Qu X, Zhu W, Li YS, Yuan S, Zhang H *et al.* Deterministically patterned biomimetic human iPSC-derived hepatic model via rapid 3D bioprinting. *Proc Natl Acad Sci U S A* 2016; **113**: 2206–2211.

131 Duarte Campos DF, Lindsay CD, Roth JG, LeSavage BL, Seymour AJ, Krajina BA *et al.* Bioprinting Cell- and Spheroid-Laden Protein-Engineered Hydrogels as Tissue-on-Chip Platforms. *Front Bioeng Biotechnol* 2020; **8**: 1–13.

132 Kolesky DB, Homan KA, Skylar-Scott MA, Lewis JA. Three-dimensional bioprinting of thick vascularized tissues. *Proc Natl Acad Sci U S A* 2016; **113**: 3179–3184.

133 Kolesky DB, Truby RL, Gladman AS, Busbee TA, Homan KA, Lewis JA. 3D bioprinting of vascularized, heterogeneous cell-laden tissue constructs. *Adv Mater* 2014; **26**: 3124–3130.

134 Homan KA, Kolesky DB, Skylar-Scott MA, Herrmann J, Obuobi H, Moisan A *et al.* Bioprinting of 3D Convoluted Renal Proximal Tubules on Perfusable Chips. *Sci Rep* 2016; **6**: 1–13.

135 Lin NYC, Homan KA, Robinson SS, Kolesky DB, Duarte N, Moisan A *et al.* Renal reabsorption in 3D vascularized proximal tubule models. *Proc Natl Acad Sci U S A* 2019; **116**: 5399–5404.

136 Miller JS, Stevens KR, Yang MT, Baker BM, Nguyen DHT, Cohen DM *et al.* Rapid casting of patterned vascular networks for perfusable engineered three-dimensional tissues. *Nat Mater* 2012; **11**: 768–774.

137 Zhu W, Qu X, Zhu J, Patel S, Liu J, Wang P *et al.* Direct 3D bioprinting of prevascularized tissue constructs with complex microarchitecture. *Biomaterials* 2018; **124**: 106–115.

138 Grigoryan B, Paulsen SJ, Corbett DC, Sazer DW, Fortin CL, Zaita AJ *et al.* Multivascular networks and functional intravascular topologies within biocompatible hydrogels. *Science (80- )* 2019; **364**: 458–464.

139 Lee VK, Kim DY, Ngo H, Lee Y, Seo L, Yoo SS *et al.* Creating perfused functional vascular channels using 3D bio-printing technology. *Biomaterials* 2014; **35**: 8092–8102.

140 Zhao L, Lee VK, Yoo SS, Dai G, Intes X. The integration of 3-D cell printing and mesoscopic fluorescence molecular tomography of vascular constructs within thick hydrogel scaffolds. *Biomaterials* 2012; **33**: 5325–5332.

141 Zhu W, Qu X, Zhu J, Patel S, Liu J, Wang P *et al.* Direct 3D bioprinting of prevascularized tissue constructs with complex microarchitecture. *Biomaterials* 2017; **124**: 106–115.

142 Datta P, Ayan B, Ozbolat IT. Bioprinting for vascular and vascularized tissue biofabrication. *Acta Biomater* 2017; **51**: 1–20.

143 Bang S, Lee S, Ko J, Son K, Tahk D. A Low Permeability Microfluidic Blood-Brain Barrier Platform with Direct Contact between Perfusable Vascular Network and Astrocytes. *Sci Rep* 2017; : 1–10.

144 Lee W, Lee V, Polio S, Keegan P, Lee JH, Fischer K *et al.* On-demand three-dimensional freeform fabrication of multi-layered hydrogel scaffold with fluidic channels. *Biotechnol Bioeng* 2010; **105**: 1178–1186.

145 Lee VK, Lanzi AM, Ngo H, Yoo SS, Vincent PA, Dai G. Generation of multi-scale vascular network system within 3D hydrogel using 3D bio-printing technology. *Cell Mol Bioeng* 2014; **7**: 460–472.

146 Kim S, Lee H, Chung M, Jeon NL. Engineering of functional, perfusable 3D microvascular networks on a chip. *Lab Chip* 2013; **13**: 1489–1500.

147 Park YC, Zhang C, Kim S, Mohamedi G, Beigie C, Nagy JO *et al.* Microvessels-on-a-chip to assess targeted ultrasound-assisted drug delivery. *ACS Appl Mater Interfaces* 2016; **8**: 31541–31549.

148 Wang X, Phan DTT, Sobrino A, George SC, Hughes CCW, Lee AP. Engineering anastomosis between living capillary networks and endothelial cell-lined microfluidic channels. *Lab Chip* 2016; **16**: 282–290.

149 Song JW, Munn LL. Fluid forces control endothelial sprouting. *Proc Natl Acad Sci U S A* 2011; **108**: 15342–15347.

150 Kim S, Chung M, Ahn J, Lee S, Jeon NL. Interstitial flow regulates the angiogenic response and phenotype of endothelial cells in a 3D culture model. *Lab Chip* 2016; **16**: 4189–4199.

151 Nguyen DHT, Stapleton SC, Yang MT, Cha SS, Choi CK, Galie PA *et al.* Biomimetic model to reconstitute angiogenic sprouting morphogenesis in vitro. *Proc Natl Acad Sci U S A* 2013; **110**: 6712–6717.

152 Chen YC, Lin RZ, Qi H, Yang Y, Bae H, Melero-Martin JM *et al.* Functional human vascular network generated in photocrosslinkable gelatin methacrylate hydrogels. *Adv Funct Mater* 2012; **22**: 2027–2039.

153 Chiu LLY, Montgomery M, Liang Y, Liu H, Radisic M. Perfusable branching microvessel bed for vascularization of engineered tissues. *Proc Natl Acad Sci U S A* 2012; **109**. doi:10.1073/pnas.1210580109.

154 Yeon JH, Ryu HR, Chung M, Hu QP, Jeon NL. In vitro formation and characterization of a perfusable three-dimensional tubular capillary network in microfluidic devices. *Lab Chip* 2012; **12**: 2815–2822.

155 Sobrino A, Phan DTT, Datta R, Wang X, Hachey SJ, Romero-López M *et al.* 3D microtumors in vitro supported by perfused vascular networks. *Sci Rep* 2016; **6**: 1–11.

156 Phan DTT, Wang X, Craver BM, Sobrino A, Zhao D, Chen JC *et al.* A vascularized and perfused organ-on-a-chip platform for large-scale drug screening applications. *Lab Chip* 2017; **17**: 511–520.

157 Ko J, Lee Y, Lee S, Lee S, Jeon NL. Human Ocular Angiogenesis-Inspired Vascular Models on an Injection-Molded Microfluidic Chip. *Adv Healthc Mater* 2019; **1900328**: 1–10.

158 Lee Y, Choi JW, Yu J, Park D, Ha J, Son K *et al.* Microfluidics within a well: An injection-molded plastic array 3D culture platform. *Lab Chip* 2018; **18**: 2433–2440.

159 Lee SR, Hyung S, Bang S, Lee Y, Ko J, Lee S *et al.* Modeling neural circuit, blood-brain barrier, and myelination on a microfluidic 96 well plate. *Biofabrication* 2019; **11**. doi:10.1088/1758-5090/ab1402.

160 Breiner KM, Schaller H, Knolle PA. Endothelial cell-mediated uptake of a hepatitis B virus: A

new concept of liver targeting of hepatotropic microorganisms. *Hepatology* 2001; **34**: 803–808.

161 Øie CI, Wolfson DL, Yasunori T, Dumitriu G, Sørensen KK, McCourt PA *et al.* Liver sinusoidal endothelial cells contribute to the uptake and degradation of entero bacterial viruses. *Sci Rep* 2020; **10**: 1–9.

162 Park JY, Ryu H, Lee B, Ha D, Ahn M, Kim S *et al.* Development of a functional airway-on-a-chip by 3D cell printing. *Biofabrication* 2019.